USE OF THE TRANSIENT RESPONSE PROFILES IN DETERMINING THE SPREADABILITY OF A SPECIFIC CREAM CHEESE , LINERA

A THESIS SUBMITTED TO
THE GRADUATE SCHOOL OF NATURAL AND APPLIED SCIENCE
OF
THE MIDDLE EAST TECHNICAL UNIVERSITY

BY

REFİK BERKAN GÜNEY

IN PARTIAL FULFILLMENT OF THE REQUIREMENTS FOR THE DEGREE OF

MASTER OF SCIENCE

IN

THE DEPARTMENT OF FOOD ENGINEERING

JANUARY 1997

Approval of the Graduate School of Natural and Applied Sciences

Prof. Dr. Tayfur Öztürk
Director

I certify that this thesis satisfies all the requirements as a thesis for the degree of Master of Science.

Prof. Dr. Faruk Bozoğlu
Head of Department

This is to certify that we have read this thesis and that in our opinion it is fully adequate, in scope and quality, as a thesis for the degree of Master Science.

Assoc. Prof. Dr. Zeynep Katnaş
Supervisor

Examining Committee Members

Assoc. Prof. Dr. Alev Bayındırlı

Assoc. Prof. Dr. Zeynep Katnaş

Assist. Prof. Dr. Ufuk Bakır

Assist. Prof. Dr. Kırali Mürtezaoğlu

Assist. Prof. Dr. Esra Yener

ABSTRACT

USE OF THE TRANSIENT RESPONSE PROFILES IN DETERMINING THE SPREADABILITY OF A SPECIFIC CREAM CHEESE, LINERA

Güney, Refik Berkan

M.S., Department of Food Engineering

Supervisor: Assoc. Prof. Dr. Zeynep Katnaş

January 1997, 77 pages

The main objective of the present study is to suggest an analytical solution to the free surface flow of a certain type of high moisture content cream cheese (Linera) which can further be developed to predict the relative spreadabilities of viscoelastic materials which exhibit negligibly low yield stress. For this purpose, the similarity between the experimental transient response profiles and the solution to the 1-D heat conduction in a slab with constant generation rate together with a linear position-dependent initial condition and linear time-dependent boundary conditions was made use of. Dimensionless analysis was carried out so as to suggest the

analogous momentum transport parameters for the parameters which exist in the solution of the heat transfer problem.

As a result it was concluded that the analogy can be used to simulate the transient response profiles except for the initial stages of the flow which can be perfected by using a more complex dependence between time and boundary conditions than linear. Dimensionless analysis proved that the parameters of the momentum transport problem are related with the momentum generation rate revealing interrelationships between gravitational, pressure and inertial effects.

Keywords: Cream cheese, Spreadability, Free Surface Flow, Dimensionless Analysis, Non-Newtonian Fluids, Yield Stress, Viscoelasticity

ÖZ

ÖZEL BİR ÇEŞİT KREM PEYNİR OLAN LİNERA DA YAYILABİLİRLİĞİN GEÇİCİ YÜZEY PROFİLLERİNİN KULLANARAK BULUNMASI

Güney, Refik Berkan

Yüksek Lisans, Gıda Mühendisliği Bölümü

Tez Yöneticisi: Doç. Dr. Zeynep Katnaş

Ocak 1997, 77 sayfa

Bu çalışmanın ana amacı, ileride yapılacak deneysel çalışmalar ile desteklendiğinde, karşı koyma stresi (yield stress) yok denecek kadar az olan vizkoelastik materyellerin göreceli yayılganlığını öngörebilecek nitelikte bir matematiksel modelin, yüksek nem içerikli bir çeşit krem peynirinin (Linera) serbest yüzey akışı için geliştirilmesidir. Bu amaçla Linera'nın serbest yüzey akışı ile, Kartezyen koordinat sisteminde, sabit ısı üretimi ile pozisyona doğrusal biçimde bağlı başlangıç zaman koşulu ve zamana doğrusal biçimde bağlı sınır koşulları içeren tek

boyutlu bir ısı aktarım problemi arasında bir analoji kuruldu. Isı aktarım problemindeki parametreleri momentum aktarımındaki eşdegerlerini bulmak amacıyla boyutsal analiz yöntemi uygulandı.

Yapılan bu çalışmanın sonucunda, bu yaklaşımın karşı koyma stresi yok denecek kadar az vizkoelastik materyellerin geçici durum tepki profillerinin çıkarılmasında kullanılabileceği, yanlız başlangıçtaki zaman aralıkları için deneysel sonuçlarla teorik öngörüler arasında farklılıklar gözlenmiştir. Düşük zaman aralıklarında daha iyi sonuçlar elde edebilmek için sınır koşullarının zamana bağımlılığı için doğrusaldan daha karmaşık ilişkiler kullanılmalıdır. Boyutsal analiz sonuçları momentum aktarım problemindeki parametrelerin yer çekimi, basınç ve eylemsizlik arasındaki karmaşık ilişkileri tanımlayan momentum üretim hızına bağlı parametreler olduğunu kanıtlamıştır.

Anahtar Kelimeler: Krem Peyniri, Yayılabilirlik, Serbest Yüzey Akışı, Boyutsal Analiz, Newton-dışı Akışlar, Karşı Koyma Stresi, Vizkoelastisite

ACKNOWLEDGEMENTS

I wish to express sincere appreciation to my thesis supervisor Assoc. Prof. Dr. Zeynep Katnaş for her invaluable supervision and guidance and to Prof. Dr. Ali Esin for his encouragement throughout the progress of my thesis.

I also wish to thank to Research Assistant Miss.Göknur Bayram for her help in viscosity determination and Research Assistant Mr. Emin Okumuş for his encouragement.

Finally, I am deeply grateful to my family for their support.

TABLE OF CONTENTS

LIST OF TABLES

TABLE

LIST OF FIGURES

FIGURES

LIST OF SYMBOLS

a = A constant in initial condition of the model equation

A_0 = Constant heat generation

A_1 = Constant

A_2 = Constant

b = A constant in boundary condition of the model equation

B_1 = Constant

B_2 = Constant

c = A constant in boundary condition of the model equation

C = Torque exerted

D = Width of the glass container

D = Diameter

erf (x) = Error function of x

erfc (x) = Complementary error function of x

g = Gravitational acceleration

h = Gap width between the plates in viscometer

k_1 = Diffusivity in heat equation

k_1 = A parameter in the model equation

k_2 = Conductivity in heat equation

k_3 = A parameter in the model equation

K = Consistency index

K_c = Constant

K_{oc} = Constant

L = Length of the container

L = Column heigth in capillary flow viscometer

n= The flow behavior index

N_x = Dimensionless number of x (x can be Re,Eu, ...)

P = Pressure

ΔP = Pressure difference

Q = Flow Rate

r = Radius

t = Time

T = Temperature

T = Torque per unit area

V = Volume (m^3)

V = Average Velocity

V_y = Velocity in y direction

$W_{container}$ = Weight of the container

x = Position in x-direction

y = Position in y-direction

y_0 = A parameter in initial condition of the model equation

y_1 = A parameter in boundary condition of the model equation

y_2 = A parameter in boundary condition of the model equation

Greek Letters;

ρ = Density

τ = Shear Stress

τ_e = Equilibrium shear stress

τ_w = Shear Stress at wall

τ_o = Yield Stress

$\dot{\gamma}$ = Shear Rate

$\dot{\gamma}_p$ =Shear Rate at the plate

λ = Structural parameter

η= Viscosity

η_a = Apparent viscosity

η' = Plastic viscosity

θ = Cone angle in radians

π = Number of pi

μ = Constant Viscosity

Ω = Angular velocity

CHAPTER 1

INTRODUCTION

1.1 The Scope

The rheological characterization of cheese is important as a means of determining body and texture (Konstance and Holsinger, 1992). One of the most important rheological properties of process cheeses is spreadability which is especially important for cream cheese (Nolan and Holsinger, 1989; Moskowitz, 1987). Spreadability is a subjective term related with yield stress and apparent viscosity. The rheological behavior of cream cheeses have been modelled by empirical equations (Kokini and Dickie, 1982; Mason et al., 1982; Massaguer-Roig et al., 1984). Also, the apparent viscosity of cream cheeses were found to decrease with increasing moisture content (Jao et al., 1981).

In the present study, the rheological behavior of a high moisture content cream cheese, Linera, which experiences free surface flow was investigated analytically through the free surface flow characteristics. When compared with the data given in the literature, the free surface flow approach is the first attempt to

suggest an analytical model for the evaluation of spreadability for viscoelastic materials which have negligibly low yield stress.

1.2 Objectives

The main objective of the present study is to suggest an analytical solution to the free surface flow of a certain type of high moisture content cream cheese (Linera) which can further be developed to predict the relative spreadabilities of viscoelastic materials which exhibit negligibly low yield stress. Specifically, it was aimed to suggest an analytical solution to the complex free surface flow phenomena for which the numerical solution is highly computer-time and computer-memory extensive due to the time- and position-dependent boundary conditions. For this purpose, the similarity between the experimental transient response profiles and the solution to the 1-D heat conduction in a slab with constant generation rate together with a linear position-dependent initial condition and linear time-dependent boundary conditions was made use of. Dimensionless analysis was carried out so as to suggest the analogous momentum transport parameters for the parameters which exist in the solution of the heat transfer problem.

CHAPTER 2

GENERAL BACKGROUND

2.1 Importance of Rheology in the Food Industry

Rheology is the science of deformation and flow of matter. The term 'rheology' was invented by E.C. Bingham in 1929 and is commonly applied to the study of liquid and liquid-like materials. However, it is also applied to solid-like materials that deform and / or flow under an applied shear stress (Tanner, 1985).

Rheological properties are important in the design of flow processes, in quality control, in storage and processing stability measurements, in predicting texture, in correlation with sensory evaluation (Davis, 1973). Rheological studies become particularly useful when predictive relationships for rheological properties of foods can be developed which start from the molecular architecture of the constituent species (Heldman and Lund, 1992).

Reliable and accurate steady rheological data are necessary for the design of continuous-flow processes such as sizing of pumps and other fluid-moving machinery and to evaluate heating rates during such engineering operations as aseptic processing and concentration (Rao, 1977a; Steath, 1976). Also rheological properties

of food materials are important in estimating the velocity, shear, and residence-time distributions in extrusion and continuous mixing (Heldman and Lund,1992).

2.1.1 The Importance of Rheology in the Cheese Industry

In the broadest classification, cheese can be grouped as natural cheese and process cheese. Cheese made directly from milk is classified as natural cheese. Process cheeses are made by blending and heating one or more varieties of natural cheeses. Process cheeses are further subdivided into pasteurized process cheeses, cheese foods, and cheese spreads (Desrosier, 1977).

Pasteurized process cheese is prepared by comminuting and mixing, a variety of cheeses and emulsifying salts by the aid of heat. Cheddar cheese is an example for this group. When certain optional dairy ingredients such as cream, skim milk, whey, or their solids are added to the cheese blend and processed, the product is called a pasteurized process cheese food or a pasteurized process cheese spread depending on its spreadability (Desrosier, 1977). Process cheese spread is characterized by an abrupt change from semi-solid to liquid depending on its composition (Moskowitz, 1987). The cream cheese, a popular North American product manufactured from cream or mixtures of milk and cream, is an example to pasteurized process cheese spread and American process cheese (Mozzarella) is an example to cheese food (Kalab and Modler, 1985).

The rheological characterization of cheese is important as a means of determining body and texture for quality and identity as well as a means of studying its structure as a function of composition, processing techniques and storage

conditions (Konstance and Holsinger, 1992). The most important functional rheological properties of cheese are its meltability, stretchability and spreadability. Meltability and stretchability properties of cheese are influenced by composition and by the plasticizing and kneading process to which the curd is subjected during manufacture (Nolan and Holsinger, 1989). Spreadability, is important for pasteurized process cheese spreads, especially cream cheese. Spreadability of cream cheese permits its use on a variety of popular solid foods such as sandwiches and snack foods (Moskowitz, 1987).

2.2 Rheology of Liquid Foods

2.2.1 Classification of Liquid Foods

Generally, liquids are classified into two categories as Newtonian and non-Newtonian liquids. A liquid which obeys the constitutive equation given below

$$\tau = \eta \dot{\gamma} \tag{2.1}$$

where τ is the shear stress, $\dot{\gamma}$ is the shear rate and the ratio of the shear stress to shear rate is defined as the viscosity, η, is called a 'Newtonian' liquid. All other liquids not showing this simple 'ideal' flow behavior are referred as 'non-Newtonian'.

The viscosity function, η, can be used to classify the flow behavior of several foods. The viscosity of Newtonian foods is influenced by only temperature and

composition and it is independent of the shear rate and previous shear history (Geankoplis 1983). Foods known to be Newtonian are listed in Table 2.1

Fluids that do not follow Newtonian behavior are called non-Newtonian fluids. The flow properties of non Newtonian fluids are influenced by the shear rate. For non-Newtonian fluids, the apparent viscosity, η_a, is used instead of the Newtonian viscosity, η, where η_a is defined as the ratio of the shear stress to the shear rate ($\eta_a=\tau/\dot{\gamma}$) (Geankoplis, 1983).

Moreover, non-Newtonian foods can be divided into two categories: time independent and time dependent. At a constant temperature, η_a for those which have time-independent apparent viscosity depends only on the shear rate, while it also depends on the duration of shear for those materials which have time dependent apparent viscosity. Time-independent flow behavior can be divided into shear-thinning (pseudoplastic) and shear-thickening (dilatant) categories, depending upon

Table 2.1 Example of Newtonian foods (Rao, 1977a)

Milk	Most honeys
Total solids, 8.36-29.07%	
Clear fruit juices	Egg products
Depectinized apple juice (15-75^0 brix)	Whole egg (unfrozen)
Filtered orange juice (10-18^0 brix)	Stabilized egg white
Concord grape juice (15-50^0 brix)	Plain yolk
Corn syrups	Sucrose solutions

whether η_a decreases or increases, respectively, with an increase in shear rate (Rao and Rizvi, 1986). A large number of non-Newtonian fluid foods exhibit pseudoplastic behavior (Table 2.2). One physical interpretation of this phenomenon is that with increasing rates of shear the molecules (or the structure) are progressively aligned (Tanner, 1985). Figure 2.1 illustrates the flow curves of Newtonian and time-independent non -Newtonian fluids.

Shear-thickening foods are rarely encountered. Pryce-Jones (1953) observed shear-thickening behavior for honey from Eucalyptus ficifolia. Bagley and Chiristianson (1982) observed shear-thickening behavior for cooked starch suspensions.

Non-Newtonian foods with time-dependent flow properties are subdivided into thixotropic and rheopectic fluids. In the case of the former, at a fixed shear rate, the viscosity decreases with time; for the latter, the viscosity increases with

Table 2.2 Examples of Shear-thinning Foods (Rao, 1977a)

Concentrated fruit juices	Dairy cream
Undepectinized apple juice 50-65 brix	Thawed frozen whole egg
Passion fruit juice 15.6-33.4 brix	Unmixed egg white
Orange juice 60-65 brix	Fruit and vegetable purees
French mustard	Gum solutions-high concentrations
Melted chocolate	Protein concentrates
Cream cheese	Peanut butter

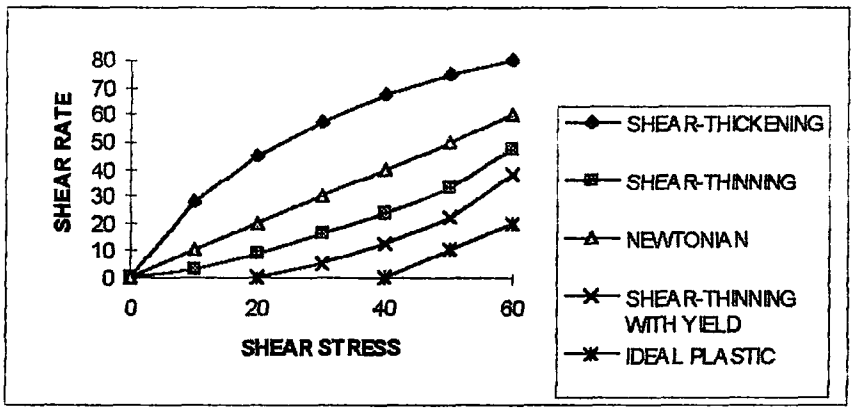

Figure 2.1 Newtonian and time-independent non-Newtonian fluids. (Rao, 1977a)

time. Thixotropic behavior has been noted for condensed milk (Higgs and Norrington, 1971), mayonnaise (Tiu and Boger, 1974; Figoni and Shoemaker, 1983), and egg white (Tung et al., 1970). Rheopectic foods have not been reported thus far.

Thixotropic materials are those whose consistency depends on the duration of shear as well as on the rate of shear (Figure 2.2). If a thixotropic material is sheared at a constant rate after a period of rest, the structure will be progressively broken down and the viscosity will decrease with time. The rate of breakdown of structure during shearing at a given rate will depend on the number of structural linkages available for breaking and must therefore decrease with time. The simultaneous rate of reformation of structure will increase with time as the number of possible new linkages increases. Eventually a state of dynamic equilibrium may be reached when the rate of build-up of structure equals the rate of breakdown (Tanner, 1985).

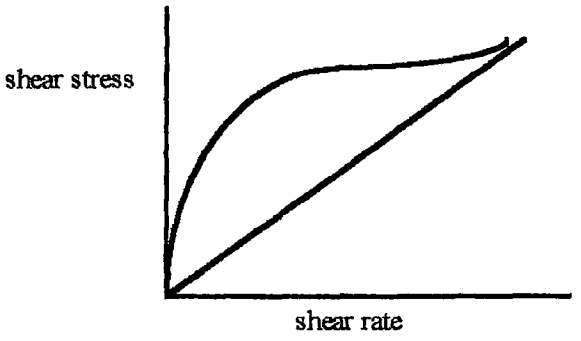

Figure 2.2 The Diagram of Thixotropy (Tanner, R. I., 1985)

2.2.2 Measurement of the Flow Properties of Liquid Foods

The instruments for measuring the flow properties of liquid foods can be classified into the following categories: fundamental, empirical, and imitative.

2.2.2.1 Fundamental Methods

Fundamental tests measure well-defined properties, utilizing geometries that are amenable to the analysis of fluid flow. Several instruments are employed for measuring the flow properties via fundamental methods; some of these are available commercially. Although many commercial instruments have been designed for application to materials other than foods, they may be used for studying liquid foods as well. It appears that the word 'viscometer' is used for an instrument designed solely to provide information on the viscosity function, whereas the word 'rheometer' is used when an instrument can also provide information on other

rheological parameters such as those related with the viscoelastic behavior (Rao and Rizvi, 1986).

The fundamental methods can be classified under the specific geometry employed: capillary, Couette (concentric cylinder), plate and cone, and parallel plate. The requirements common to all these geometries can be summarized as; steady laminar flow of the fluid, isothermal operation, and no slip at solid-fluid interfaces.

2.2.2.1.1 Capillary Flow

Capillary viscometers made of glass and operating under gravity are used mainly for Newtonian liquids. For non-Newtonian fluids, the design must allow operation over a wide range of flow rates, and the shear stress must be determined for fully developed flow conditions (Rao and Rizvi, 1986). Figure 2.3 illustrates capillary flow for use in a viscometric system.

The shear stress and shear rate at the wall can be determined from Eqs. (2.2) and (2.3), respectively (Brodkey, 1967) :

$$\tau_w = \frac{D\Delta P}{4L} \tag{2.2}$$

$$\left(\frac{dv}{dr}\right)_w = \frac{3}{4}\left(\frac{32Q}{\pi D^3}\right) + \frac{\tau_w}{4}\frac{d(32Q/(\pi D^3))}{d(\tau_w)} \tag{2.3}$$

For a capillary aligned vertically, the measured pressure drop must be corrected for the column of liquid of height L. In situations where the pressure drop cannot be determined for fully developed flow conditions, corrections for the undeveloped flow conditions (end effects) must be made (Bagley, 1957).

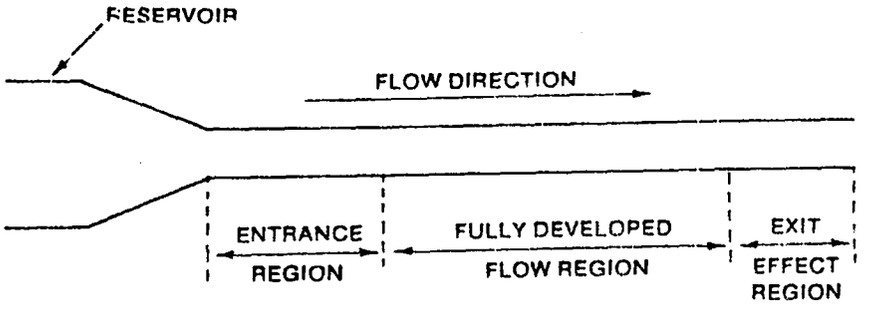

Figure 2.3 Capillary Flow Viscometer (Rao and Rizvi, 1986)

The flow behavior of a variety of food suspensions have been studied by utilizing tubes having diameters of 6-10 mm (Vitali and Rao, 1982). The advantages of the capillary viscometer are its usage in a wide range of shear rates and its suitability to suspensions with relatively large particles.

2.2.2.1.2 Couette Flow Viscometer

A number of Couette (concentric cylinder) viscometers (Figure 2.4) are available commercially (Van Wazer et al. , 1963; Whorlow, 1980). Either the outer or the inner cylinder can be rotated. For the case of the outer cylinder rotating and the inner cylinder stationary, it can be shown that (Brodkey, 1967):

$$2\tau_i \frac{d\Omega}{d\tau_i} = \gamma_i - \gamma_0 \qquad (2.4)$$

where Ω is the angular velocity of the outer cylinder (radians/second), γ is the shear rate, and the subscripts i and 0 denote the inner and outer cylinders, respectively.

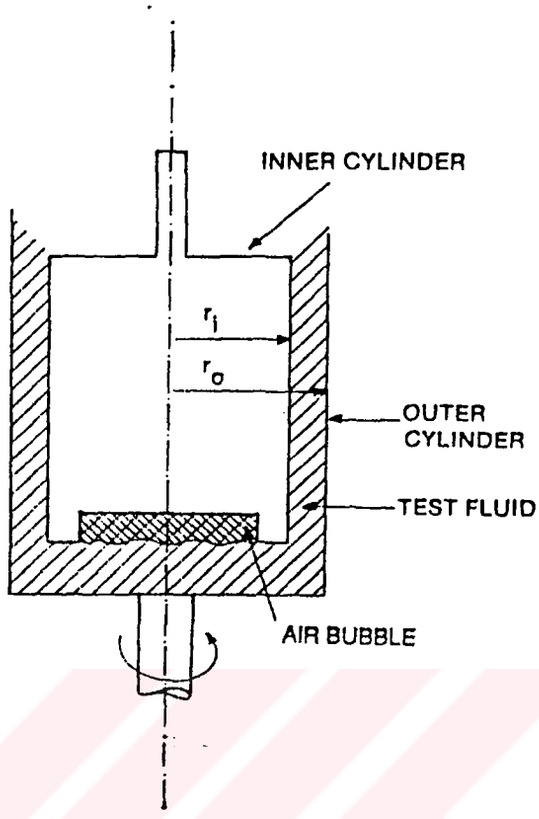

Figure 2.4 Concentric Cylinder Viscometer (Rao and Rizvi, 1986)

Couette, cone-and-plate and parallel plate viscometers are referred to as the narrow gap viscometers which are limited to relatively low shear rates. At high shear rates end effects arising from the inertia of the sample and secondary flows generated due to fluid inertia make rheological measurements invalid. In addition to those narrow gap viscometers are not suitable for suspensions which contain particulate matter comparable in size with the gap between the plates.

2.2.2.1.3 Plate and Cone Viscometers

As the name indicates, a plate and cone viscometer consists of a circular flat plate and a cone (Figure 2.5). For the case of a fixed plate and a rotating cone with a small angle, Brodkey (1967) showed that:

$$\tau_p = \frac{3T}{D} \tag{2.5}$$

$$\dot{\gamma}_p = \frac{\Omega}{\theta} \tag{2.6}$$

where τ_p is the shear stress at the plate, T is the torque per unit area, D is the plate diameter, Ω is the angular velocity, $\dot{\gamma}_p$ is the shear rate at the plate, and θ is the cone angle in radians. The limitation to the usage of suspensions having large particle is the most effective for the cone and plate geometry where the tip of the cone is almost in touch with the plate (Heldman and Lund, 1992).

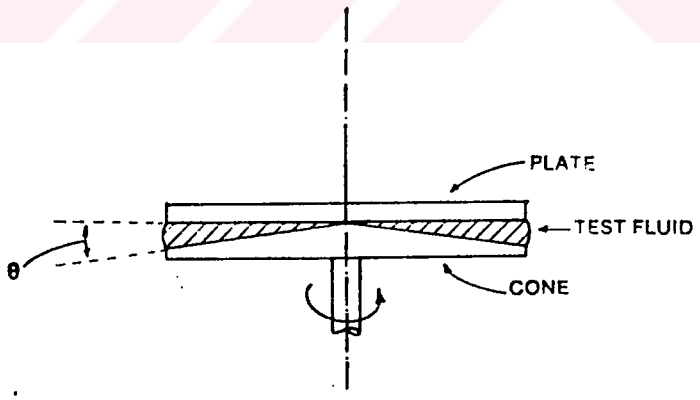

Figure 2.5 Plate and Cone System (Rao and Rizvi, 1986)

2.2.2.1.4 Parallel Plate Geometry

Instead of a plate and cone system, a parallel plate geometry can also be used (Figure 2.6). The pertinent equations for the shear rate ($\dot{\gamma}$) and the shear stress (τ) are (Walters, 1975):

$$\dot{\gamma} = \Omega \frac{r}{h} \tag{2.7}$$

$$\tau = \frac{3C}{2\pi r^3}\left(1 + \frac{1}{3}\frac{d\ln C}{d\ln \dot{\gamma}}\right) \tag{2.8}$$

where Ω is the angular velocity, r is the radius, h is the gap width between the plates, and C is the torque exerted. The limitations to the usage of suspensions for narrow gap viscometers may be overcome in the plate geometry by increasing the size of the gap. However, it should still be guaranteed that the gap opening is much smaller

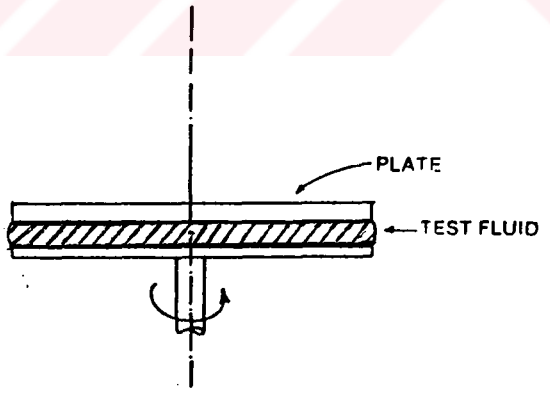

Figure 2.6 Parallel Plate Geometry

than the plate radius. The parallel plate geometry is particularly useful to understand structure-rheology relationships because of its effectiveness in low shear rates. In the present study, the parallel plate type viscometer was used in determining the rheological behavior of Linera.

2.2.2.2 Empirical Methods

Rotational viscometers with spindle geometries that are difficult to analyze mathematically have been employed in the empirical tests. The geometries include spindles with protruding pins and flags. These geometries are available from the manufacturers of the rotational viscometers: Brookfield, Haake, and Epprecht Rheomat. Utilizing these geometries, one obtains for non-Newtonian liquids a magnitude of apparent viscosity in arbitrary units. The use of these complex geometries has been limited to quality control purposes.

These instruments are used to measure the consistency of pureed foods. The word 'consistency' is used with the understanding that it is a property related to the apparent viscosity of suspensions. Adams consistometer, Bostwick consistometer and Efflux tube viscometer are examples to instruments of empirical methods (Rao, 1977b).

2.2.2.3 Imitative Methods

In the case of imitative methods, the properties are measured under test conditions that simulate those in practice. There are several instruments that perform

imitative tests, and most of these are applicable to solid-like food materials. Examples of instruments that perform imitative tests are butter spreaders, the General Foods Texturometer, and the Brabender Farinograph (White, 1970).

2.2.3 Rheological Models for Liquid foods

2.2.3.1 Models for Time-Independent Behavior

The power law model with or without a yield term (Eqs. (2.9) and (2.10)) has been employed extensively to describe the flow behavior of viscous foods over wide ranges of shear rates (Vitali and Rao, 1984):

$$\tau = K\dot{\gamma}^{n} \tag{2.9}$$

$$\tau - \tau_0 = K\dot{\gamma}^{n} \tag{2.10}$$

where τ_0 is the yield stress, K is the consistency index and n is the flow behavior index. Eq. (2.10) is also known as the Herschel-Bulkley model (Brodkey, 1967).

The Casson (1959) model (Eq. 2.11) has been used for foods, particularly for estimating the yield stress:

$$\tau^{0.5} - K_{oc} = K_c\dot{\gamma}^{0.5} \tag{2.11}$$

where K_{oc} and K_c are constants. The magnitude of $K_{oc}^{\ 2}$ has been used as the yield stress by a number of workers (Charm, 1963; Tung et al., 1970; Rao et al., 1981). It seems that for a number foods, such as tomato paste and concentrated orange juice, the Casson yield stress is much higher than either that predicted by the Herschel-

Bulkley model (Eq. (2.10)) (Rao and Cooley, 1983) or than that determined experimentally (Vitali and Rao, 1984).

The Bingham model (Eq. (2.12)) has been employed for describing the flow behavior of apricot puree (Schaller and Knorr, 1973) and minced fish paste (Nakayama et al., 1980) :

$$\tau - \tau_0 = \eta' \dot{\gamma} \tag{2.12}$$

where η' is the plastic viscosity.

Among the aforementioned models, the power law model (Eq. (2.10)) has been employed extensively for characterizing foods, including shear-thinning foods.

As indicated by Eqs. (2.10-12), the common feature of all these empirical models is the yield stress which can be defined as the applied stress required to initiate shear flow (Campanella and Peleg, 1987). The determination of the yield stress in semi-liquid foods can be done by various direct or indirect methods. In general, the direct methods are based on a gradual and controlled increase of the stress until flow can be detected or by measuring the residual stress after a sheared specimen is let relax (Van Wazer et al., 1963; Mizrahi and Berk, 1972; Balmaceda et al., 1973).

The indirect methods are usually based on fitting the flow curve with a model that includes a yield stress term and calculating its magnitude from statistical regression. The most popular models for such calculations are the Herschel-Bulkley model given by Eq. (2.9) and the Casson model given by Eq. (2.11). One difficulty with such indirect methods is that the magnitude of the calculated yield stress may depend on the selected model (Barbosa and Peleg, 1983). Similarly, direct

extrapolation of the flow curve itself to zero shear rate may also introduce an element of arbitrariness to the yield stress determination.

According to Mewis (1980) and Bagley (1983) one of the most sensitive methods of yield stress determination is from a plot of the apparent viscosity vs the shear stress. In this form the viscosity tends to infinity when the yield stress value is reached. Application of this method was reported by Mills and Kokini (1984) in Karaya gum dispersion and Gencer and Peleg (1984) in tomato paste and gum mixtures. The results showed that yield stress could be independently determined. Also in the present study, apparent viscosity vs shear stress plot was used for the determination of the yield stress of Linera.

2.2.3.2 Rheological Models for Thixotropic Foods

Tiu and Boger (1974) employed a kinetic-rheological model to characterize the thixotropic behavior of a mayonnaise sample. It was based on the Herschel-Bulkley model (Eq. (2.12)) multiplied by a structural parameter, λ, which ranges between an initial value of unity for zero shear time to an equilibrium value, λ_e, which is less than unity:

$$\tau = \lambda(\tau_0 + K\dot{\gamma}^n) \tag{2.13}$$

The decay of the structural parameter was assumed to obey the second-order rate equation:

$$\frac{d\lambda}{dt} = -K_1(\lambda - \lambda_e)^2 \tag{2.14}$$

where K_1 is a parameter that is a function of the shear rate. If the parameters

τ_0, K, n, K_1 and λ_e are determined from experimental data, Eqs (2.13) and (2.14) can be used for the complete rheological characterization of a thixotropic food product. Tiu and Boger (1974) provided additional equations to facilitate estimation of the various parameters.

Tung et al. (1970) studied the thixotropic properties of fresh, aged and gamma-irradiated egg white. The mathematical models by Weltman (1943) (Eq. (2.15)) and by Hahn et al. (1959) (Eq. (2.16)) were used to describe the thixotropic behavior:

$$\tau = A_1 - B_1 \log t \tag{2.15}$$

$$\log(\tau - \tau_e) = A_2 - B_2 t \tag{2.16}$$

where τ_e is the equilibrium shear stress, t is the time in seconds and A_1, A_2, B_1, and B_2 are constants. The coefficients A_1 and A_2 indicate initial shear stresses, whereas the coefficients B_1 and B_2 indicate rates of structural breakdown.

2.2.3.3 Rheological Models for Viscoelastic Foods

Some liquids demonstrate both viscous and elastic properties; these liquids are called viscoelastic. Examples of viscoelastic foods are dairy cream, ice cream mix (Prentice, 1972), peanut butter and whipped butter (Dickie and Kokini, 1982). Viscoelastic materials have long relaxation times and thus exhibit shear flow behavior which is both strain and rate of strain dependent (Kokini and Dickie, 1981). To model viscoelastic behavior, the equation of Mason et al., 1982 can be used:

$$\tau = m(\dot{\gamma})^n \left[1 + (b_0 \dot{\gamma} t - 1) \sum \frac{b_i e^{-t/\lambda_i}}{\sum b_i} \right] \qquad (2.17)$$

where m and n are the familiar power law parameters, λ_i are time constants, and b_0 and b_i are constants. The term $b_0 \dot{\gamma} t$ simulates the initial growth in stress and the terms $b_i e^{-t/\lambda_i}$ can be increased to accommodate the wide spectra of possible relaxation times.

2.3 Physical Properties of Cream Cheese

The composition of cream cheese is variable depending on the type. The moisture content is usually in the range of 30-60%, milk-fat in the range of 20-40% and protein in the range of 10-20% (Kalab and Modler, 1985b). The composition of cream cheese affects its rheological behavior. Thus a variety of models has been reported to describe the flow behavior of cream cheese in the literature.

Kokini and Dickie (1982) studied modeling of transient viscoelastic flow in foods in which cream cheese was considered as viscoelastic and the model parameters were calculated using the equation by Mason et al. (1982) (Eq. (2.19)). Massaguer-Roig et al. (1984) modelled cream cheese as a thixotropic liquid. The time dependent rheological behavior was expressed by the modified form of the Herchel-Bulkley model (Eq. (2.15)).

Jao et al. (1981) studied the effect of moisture and temperature on the rheological properties of cream cheeses. They showed that the increase in moisture

content causes the reduction of apparent viscosity and leads to an increase in the shear-thinning behavior.

2.4 Spreadability of Foods

Spreadability of foods is usually assessed during spreading a semi-solid or viscous liquid food on a solid food. For example, the spreading of butter on a solid food by a knife is an example to spreadability. In that case, the spreadability is inversely proportional to the shear stress on the surface of the knife (Kokini and Dickie, 1982). Also, the spreading of a viscous liquid cream cheese on a solid food in the effect of gravitational forces is an example to spreadability. In that case, the flow occurs in the free surface. Therefore it is also an example to the free surface flow.

Many studies have been published on the spreadability of foods, most of them concentrating on the relationship between sensory and instrumental measures of spreadability. Dixon and Parekh (1977) advocated the use of a cone penetrometer for measuring spreadability because it correlated best with sensory measurements. Mortensen and Danmark (1982) felt that yield stress was a sufficient measure of spreadability. These studies tended to concentrate on instrumental rather than sensory measurements.

In 1982, Kokini and Dickie (1982) developed a model for food spreadability using the principles of fluid mechanics. Subjective spreadability was predicted through understanding of the psychophysical mechanisms involved during the back and forth spreading action of foods (apple butter, mayonnaise, soft margarine,

tomato ketchup, mustard, stick butter, tub margarine, stick margarine, whipped butter, cream cheese, desserts, honey, peanut butter and frosting) on crackers. Transient complex rheology of the food product is incorporated into mass and momentum balances used to model the spreading action where;

Torque= Shear stress on the knife × Area of the knife × Length of the knife (2.18)

$$\text{Spreadability } \alpha \frac{1}{\text{Torque on knife}} \tag{2.19}$$

Pompei et al., (1988) developed two instrumental imitative methods simulating the manual operation of spreading using the Instron equipment. The first method was based on a prototype cell (Pompei Spreadability Cell) and the other involved manual spreading of a known volume of product during which the force applied was recorded. Both methods showed high correlation with the sensory results. Lucisano et al., (1989) carried out the instrumental evaluation of hardness and spreadability by a penetration method and by the Pompei Spreadability Cell. Results obtained with these methods on water-bentonite mixtures at different concentrations were found to well correlate with the sensory evaluation of hardness and spreadability.

2.5 Free Surface Flow

The coating process is an example to the free surface flow (Tanner, 1985). In the food industry, coating of cookies with chocolate is one of the principal applications of free surface flow. Extrusion system and also the flow of melted mozzarella cheese on pizza can be considered as examples of free surface flow in

food systems. The spreading of liquid foods on solid foods freely due to the gravitational force is one of the general areas of free surface flow in food systems.

2.5.1 Mathematical Treatment of Free Surface Flow

In fluid mechanics, one of the most complicated problems is the free surface flow. It is impossible to solve the free surface flow analytically due to the complex non-linearity of the governing partial differential equations (Equations of motion). The numerical solution is also complicated due to the presence of the free surfaces which requires some means of recording the position of the free surface numerically and the imposition of the free surface boundary conditions. The shape of the free surface changes with time as a function of x and y. Thus the shape of the free surface as a function of x and y is needed at any particular time, t, which requires a trial and error procedure. Therefore, since the free surface is both time and position dependent, the location of the free surface and the free surface boundary at any particular time are dependent on each other and this situation increases the complexity of the numerical solution. Moreover, on the free surface, zero normal velocity, zero or prescribed shear stress and zero or prescribed normal stress have to be satisfied (Tanner, 1985).

In the literature, there are only a few studies for the free surface treatment of non-Newtonian flow (Kothe and Mjolsness,1992 ; Hansen and Kelman,1994). However, since the sofware suggested is of commercial value, the algorithms related with the numerical methods used are not available.

In the present study, an analytical model with analogy to heat transfer was preferred rather than a numerical solution. In the literature several studies using a similar approach have been reported. Osorio and Steffe (1984) developed a flow model for circular tubes by making use of the kinetic energy equation. The influence of yield stress, consistency coefficient and flow behavior index were investigated and the results indicated that the theoretical velocity profiles were able to simulate the experimental data. Dutta and Sastry (1990) studied the average velocities of food particle suspensions in holding tube flow. Results indicated the mean normalized velocity of particles was significantly affected by particle Froude number and a dimensionless viscosity. Meer and Fryer (1992) studied fluid flow and mixing in a cavity transfer mixer facilitating design and scale up.

2.6 The Optimization Techniques

In the present study, use of optimization techniques was required to obtain the model parameters which would simulate the free surface flow of Linera.

Optimization might be defined as the science of determining the 'best' solutions to certain mathematically defined problems, which are often models of physical reality. Mathematically, this means finding the minimum or maximum of a function of n variables, $f(x_1, , , , x_n)$, where n may be any integer greater than zero (Fletcher, 1991).

There are various methods of optimization. Any investigation seeking the optimal value of an unknown function is a search problem. Search techniques are classified into 2 groups according to the number of independent variables of the

problem; Univariable Techniques and Multivariable Techniques. The methods related to these techniques are given in Table 2.3.

In the present study, the Modified Simplex Method of Search Techniques was used for which the algorithm is given in Figure 2.7. The Simplex Method, first described by Spendley, Himsure and Hext (1962), provides a useful procedure for minimizing a given function which was further developed by Nelder and Mead (1965) . The advantages of the Nelder and Mead Simplex Method are its requirement of lower computer storage capacity and its robustness at low dimensionality. Although the method becomes less competitive as dimensionality of the objective function is raised, it is very popular relative to other multivariable search techniques.

The Nelder and Mead Simplex Method assumes the solution to exist with in a regular simplex which is a set of n+1 equidistant points in n-dimensional space. The

Table 2.3 Search Techniques for Optimization of search problem

Univariable Techniques	Multivariables Search Techniques
1. Direct Search Method	1. Alternating Variables Methods
2. Univariate Search Method	2. Pattern Search
3. Great Search Method	3. Powell's Method
4. Fibonnacci Search Method	4. EVOP Method
5. Golden Section Method	5. Modified Simplex Method
6. Quatratic Interpolation Method	

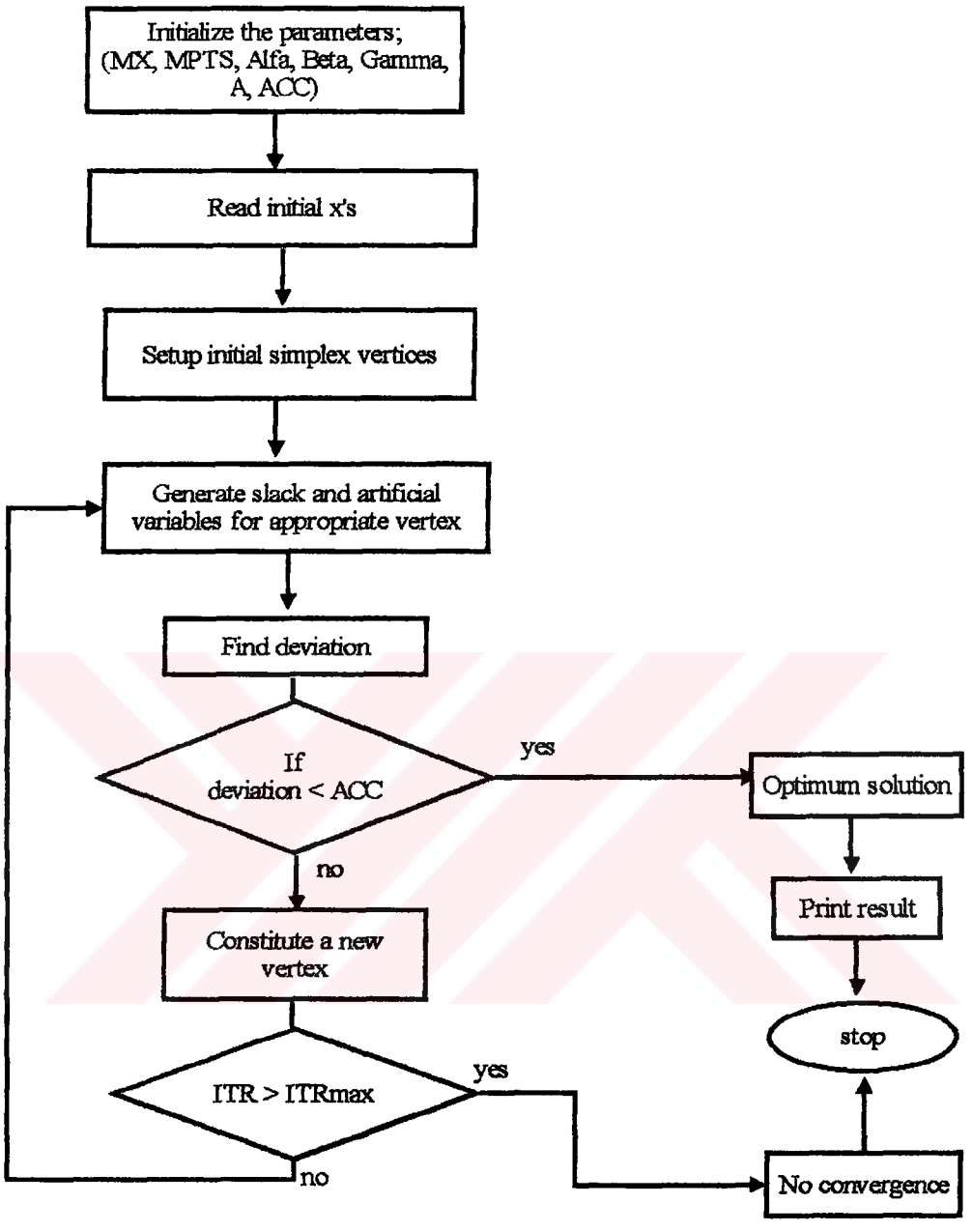

Figure 2.7 The Logic Diagram of Modified Simplex Method

current information kept in the method is the coordinates of the n+1 points and their corresponding function values.

Suppose that for iteration k the vertices of the simplex are $x_0, x_1, \ldots\ldots, x_n$ with corresponding function values $F_0, F_1, \ldots\ldots, F_n$ ordered such that

$$F_n > F_{n-1} > \ldots\ldots > F_1 > F_0 . \qquad (2.20)$$

Hence x_0 is the best vertex of the simplex and x_n is the worst. Let c be the centroid of the vertices $x_0, x_1, \ldots\ldots, x_{n-1}$, i.e.

$$c_i = \frac{1}{n}\sum_{j=0}^{n-1} x_{ji}, \quad i = 1, \ldots\ldots, n \qquad (2.21)$$

Then as in the original Simplex method (Spendly et al. ,1962) the worst vertex x_n is to be replaced and a simple reflection move is tried first, giving a new point x_r where

$$x_r = c + \alpha(c - x_n) \qquad (2.22)$$

and $\alpha > 0$ is the reflection coefficient. There are then three possible cases to be considered: x_r is a point such that $F_0 < F_r < F_{n-1}$; $F_r < F_0$ such that x_r is a new best point; $F_r > F_{n-1}$ such that x_r would be a new worst point. In the case where $F_0 < F_r < F_{n-1}$ then x_r replaces x_n and the iteration is complete.

However, if the reflection has produced a new best point, then the direction of the reflection may be a useful one so an attempt is made to expand the design along it by defining the point

$$x_e = c + \beta(x_r - c) \qquad (2.23)$$

where $\beta > 1$ is the expansion coefficient. Then if $F_e < F_0$, the expansion is considered to be successful and x_e replaces x_n; otherwise the expansion is deemed to have failed and x_n is replaced by x_r. In either event the iteration is then complete.

If the original reflection resulted in a new worst point then it is assumed that the size of the design is too large to allow any progress to be made, and so a contracted simplex is derived by defining the point x_c where

$$x_c = c + \gamma(x_n - c) \qquad \text{if } F_n < F_r \tag{2.24}$$

and

$$x_c = c + \gamma(x_r - c) \qquad \text{if } F_n > F_r, \tag{2.25}$$

and γ is the contraction coefficient with $0 < \gamma < 1$. If $F_c < \min(F_n, F_r)$ the contraction has succeeded and x_c replaces x_n; otherwise a more comprehensive contraction is carried out by halving the distances from the best point x_0 of all the other vertices of the simplex. In either case the iteration is then complete.

CHAPTER 3

EXPERIMENTAL

3.1 Material

Linera cream cheese samples produced by Unilever San. ve Tic. T.A.Ş. were purchased at a local supermarket. They were stored in their original packages in a refrigerator (6-8 ^{0}C) until sample preparation (i.e. , one day before testing).

3.2 Methods

For all the experimental techniques, the Linera samples were left overnight to equilibrate at the test temperature of 20 - 21 ^{0}C.

3.2.1 Determination of the Physical Properties

The physical properties of Linera are needed in the rheological characterization and the dimensional analysis of the momentum transport parameters

in the model equation describing free surface flow for which the details are given in Chapter 4.

3.2.1.1 Determination of Density

Density determination of Linera samples were made in a glass container (20 cm × 2 cm × 20 cm). First the empty container was weighed, then the Linera was placed in the container and weighed again. Finally, the density of Linera was calculated as

$$\rho = \frac{W_{container\ +\ cream\ cheese} - W_{container}}{V_{container}} \qquad (3.1)$$

where;

W : weight (kg)

V : volume (m^3)

3.2.1.2 Determination of Viscosity

The rheological behavior of Linera samples were determined using a HAAKE parallel plate rheometer. The set-up consists of Rotovisco RV20 with a measuring system, CV20, parallel plate sensors and a rheocontroller, RC20 coupled to a computer. The parallel plates used had a diameter of 19.25 mm and the gap width between the plates was 1 mm. The rheological measurements of Linera were carried out at steady state with a PQ20 sensor system for paralel plates. The measurements

were made at constant shear rates of 0.2, 0.32, 0.56, 0.92, 1.54, 2.58, 4.3, 7.16, 11.98 and 20.00 sec^{-1}.

In the experiments, the material was placed between the two parallel plates. The lower plate was rotated at definite rotational speeds of 0.198, 0.317, 0.554, 0.91, 1.52, 2.55, 4.25, 7.08, 11.86 and 19.84 rpm while the upper plate was held stationary and the resulting shear stress was measured. The results of the experiment are given in Appendix A.

3.2.2 Determination of the Transient Surface Profile

The transient surface profile experiments were carried out in a glass container designed and constructed for this purpose (Figure 3.1). The front and the rear

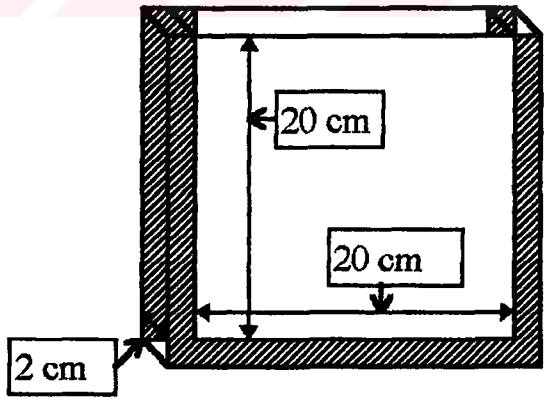

Figure 3.1 Schematic view of the glass container

surfaces of the container were made of glass and the edge of the container was made of plexi-glass.

Initially the container was half-full with Linera and positioned at a 45^0 inclined position (Figure 3.2). Then, the prop of the container was removed, and the container was placed in 90^0 position. At the same time, the chronometer was started and the transient surface profiles were measured every 150 seconds by means of a transparent graph paper placed on the surface of the container until the flow stopped with the surface profile assuming a horizontal position (Figure 3.3).

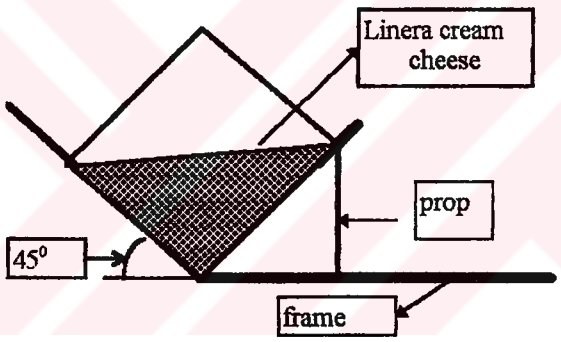

Figure 3.2 Initial state of the container

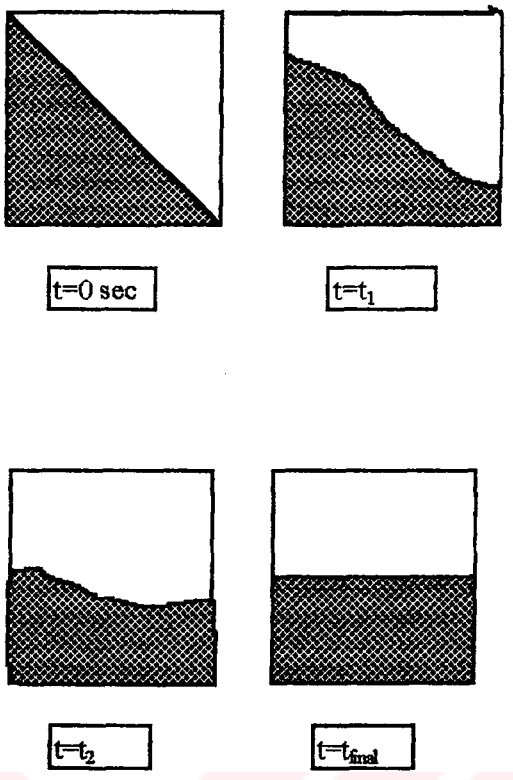

Figure 3.3 Surface profiles for the flow of Linera between initial to final states

CHAPTER 4

THEORETICAL

4.1 The Model Equation Simulating Free Surface Flow of Linera

In transport phenomena there is a proximate relationship between heat, mass and momentum transfer. In the present study, the similarity between the data taken on the surface profile during the flow of Linera and the temperature profile of unsteady state 1-Dimensional heat conduction in a slab with constant generation rate was used together with a linear position-dependent initial condition and linear time-dependent boundary conditions to propose a deterministic model predicting the surface flow of Linera.

4.1.1 The Solution of One-Dimensional Unsteady State Heat Conduction with Constant Generation in a Slab with a Linear Position-Dependent Initial Condition and Time-Dependent Linear Boundary Conditions

The differential equation to be solved is

$$\frac{\partial^2 T}{\partial x^2} - \frac{1}{k_1}\frac{\partial T}{\partial t} = -\frac{A_0}{k_2} \tag{4.1}$$

where

T: temperature (K)

k_1: thermal diffusivity ($k_2/(\rho C_p)$) (m^2/s)

k_2: thermal conductivity (W/(m-K))

A_0: constant thermal energy generation rate (W/m^3)

with the following initial (IC) and boundary conditions (BC)

$$\text{IC}: \quad T=T_0+ax \qquad x\geq 0 \qquad t=0 \tag{4.2}$$

$$\text{BC1}: \quad T=T_1+bt \qquad x=0 \qquad t>0 \tag{4.3}$$

$$\text{BC2}: \quad T=T_2+ct \qquad x=L \qquad t>0 \tag{4.4}$$

where a, b and c are constants and L is the thickness of the slab. T_0, T_1 and T_2 are initial temperatures (Figure 4.1).

By applying the Laplace transformation to Eq. (4.1),

$$\int_0^\infty e^{-pt}\frac{\partial^2 T}{\partial x^2}dt - \frac{1}{k_1}\int_0^\infty e^{-pt}\frac{\partial T}{\partial t}dt = -\frac{A_0}{k_2}\int_0^\infty e^{-pt}dt \tag{4.5}$$

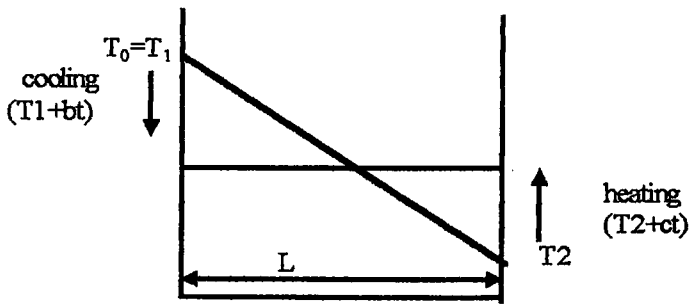

Figure 4.1 1-D Heat Conduction in a Slab

is obtained. Using the fundamental properties of Laplace transformation (Appendix B, Eq. (B.2) and Eq. (B.3)), Eq. (4.5) reduces to;

$$\frac{d^2\overline{T}}{dx^2} - \frac{p}{k_1}\overline{T} = -\frac{A_0}{k_2 p} - \frac{T_0 + ax}{k_1} \tag{4.6}$$

with the boundary conditions;

$$\overline{T} = \frac{T_1}{p} + \frac{b}{p^2} \qquad x = 0 \tag{4.7}$$

$$\overline{T} = \frac{T_2}{p} + \frac{c}{p^2} \qquad x = L \tag{4.8}$$

The complementary solution to Eq. (4.6) is

$$\overline{T}_c = C_1 e^{\sqrt{\frac{p}{k_1}}x} + C_2 e^{-\sqrt{\frac{p}{k_1}}x} \tag{4.9}$$

while the particular solution is given as;

$$\overline{T}_p = \frac{a}{p}x + \frac{A_0 k_1 / k_2}{p^2} + \frac{T_0}{p} \tag{4.10}$$

Thus the general solution of Eq. (4.6) can be written as;

$$\overline{T} = C_1 e^{\sqrt{\frac{p}{k_1}}x} + C_2 e^{-\sqrt{\frac{p}{k_1}}x} + \frac{a}{p}x + \frac{A_0 k_1 / k_2}{p^2} + \frac{T_0}{p} \tag{4.11}$$

The constants C_1 and C_2 in Eq. (4.11) can be found by applying the boundary conditions (Eq. (4.7) and Eq. (4.8)). Thus, the general solution of Eq. (4.6) becomes;

$$\overline{T} = \left(\frac{T_1 - T_0}{p}\right) e^{\sqrt{\frac{p}{k_1}}x} + \left(\frac{b - A_0 k_1 / k_2}{p^2}\right) e^{\sqrt{\frac{p}{k_1}}x} -$$

$$-\left(\frac{aL+T_0-T_2}{p}\right)\frac{e^{\sqrt{\frac{p}{k_1}}(x-L)}}{\left(1-e^{-2\sqrt{\frac{p}{k_1}}L}\right)}-\left(\frac{A_0k_1/k_2-c}{p^2}\right)\frac{e^{\sqrt{\frac{p}{k_1}}(x-L)}}{\left(1-e^{-2\sqrt{\frac{p}{k_1}}L}\right)}$$

$$-\left(\frac{T_1-T_0}{p}\right)\frac{e^{\sqrt{\frac{p}{k_1}}x}}{\left(1-e^{-2\sqrt{\frac{p}{k_1}}L}\right)}-\left(\frac{b-A_0k_1/k_2}{p^2}\right)\frac{e^{\sqrt{\frac{p}{k_1}}x}}{\left(1-e^{-2\sqrt{\frac{p}{k_1}}L}\right)}+$$

$$+\left(\frac{aL+T_0-T_2}{p}\right)\frac{e^{-\sqrt{\frac{p}{k_1}}(x+L)}}{\left(1-e^{-2\sqrt{\frac{p}{k_1}}L}\right)}+\left(\frac{A_0k_1/k_2-c}{p^2}\right)\frac{e^{-\sqrt{\frac{p}{k_1}}(x+L)}}{\left(1-e^{-2\sqrt{\frac{p}{k_1}}L}\right)}$$

$$+\left(\frac{T_1-T_0}{p}\right)\frac{e^{-\sqrt{\frac{p}{k_1}}x}}{\left(1-e^{-2\sqrt{\frac{p}{k_1}}L}\right)}+\left(\frac{b-A_0k_1/k_2}{p^2}\right)\frac{e^{-\sqrt{\frac{p}{k_1}}x}}{\left(1-e^{-2\sqrt{\frac{p}{k_1}}L}\right)}$$

$$+\frac{a}{p}x+\frac{A_0k_1/k_2}{p^2}+\frac{T_0}{p} \qquad (4.12)$$

By taking the inverse Laplace transform (Appendix C) together with the application of the binomial theorem (Appendix D), Eq. (4.12) takes the form;

$$T=(T_1-T_0)\,\mathrm{erfc}\left(\frac{-x}{2\sqrt{k_1t}}\right)$$

$$+(b-A_0k_1/k_2)\left[\left\{\left(t+\frac{(-x)^2}{2k_1}\right)\mathrm{erfc}\left(\frac{-x}{2\sqrt{k_1t}}\right)\right\}-\left\{(-x)\left(\frac{t}{\pi k_1}\right)^{1/2}e^{-(-x)^2/(4k_1t)}\right\}\right]$$

$$-(aL+T_0-T_2)\sum_{n=0}^{\infty}\mathrm{erfc}\left(\frac{-x+L(1+2n)}{2\sqrt{k_1t}}\right)-$$

$$-(A_0k_1/k_2-c)\sum_{n=0}^{\infty}\left[\left\{\left(t+\frac{(-x+L(1+2n))^2}{2k_1}\right)\operatorname{erfc}\left(\frac{-x+L(1+2n)}{2\sqrt{k_1t}}\right)\right\}-\right.$$

$$\left.\left\{(-x+L(1+2n))\left(\frac{t}{\pi k_1}\right)^{1/2}e^{-(-x+L(1+2n))/(4k_1t)}\right\}\right]$$

$$-(T_1-T_0)\sum_{n=0}^{\infty}\operatorname{erfc}\left(\frac{-x+2nL}{2\sqrt{k_1t}}\right)-$$

$$-(b-A_0k_1/k_2)\sum_{n=0}^{\infty}\left[\left\{\left(t+\frac{(-x+2nL)^2}{2k_1}\right)\operatorname{erfc}\left(\frac{-x+2nL}{2\sqrt{k_1t}}\right)\right\}-\right.$$

$$\left.\left\{(-x+2nL)\left(\frac{t}{\pi k_1}\right)^{1/2}e^{-(-x+2nL)/(4k_1t)}\right\}\right]$$

$$+(aL+T_0-T_2)\sum_{n=0}^{\infty}\operatorname{erfc}\left(\frac{x+L(1+2n)}{2\sqrt{k_1t}}\right)$$

$$+(A_0k_1/k_2-c)\sum_{n=0}^{\infty}\left[\left\{\left(t+\frac{(x+L(1+2n))^2}{2k_1}\right)\operatorname{erfc}\left(\frac{x+L(1+2n)}{2\sqrt{k_1t}}\right)\right\}-\right.$$

$$\left.\left\{(x+L(1+2n))\left(\frac{t}{\pi k_1}\right)^{1/2}e^{-(x+L(1+2n))/(4k_1t)}\right\}\right]+$$

$$+(T_1-T_0)\sum_{n=0}^{\infty}\operatorname{erfc}\left(\frac{x+2nL}{2\sqrt{k_1t}}\right)$$

$$+(b-A_0k_1/k_2)\sum_{n=0}^{\infty}\left[\left\{\left(t+\frac{(x+2nL)^2}{2k_1}\right)\operatorname{erfc}\left(\frac{x+2nL}{2\sqrt{k_1t}}\right)\right\}-\right.$$

$$\left.\left\{(x+2nL)\left(\frac{t}{\pi k_1}\right)^{1/2}e^{-(x+2nL)/(4k_1t)}\right\}\right]$$

$$+\left[(A_0k_1/k_2)t\right]+ax+T_0 \qquad (4.13)$$

4.1.2 Similarity between the Temperature Profile T(x,t) of the Slab and the Flow Profile y(x,t) of Linera

From the solution of one-dimensional unsteady state heat conduction equation (Eq. 4.1) in a slab (cooling (T_1+bt) at one side and heating (T_2+ct) at the other side) with suitable parameters,

$$a<0 \tag{4.14}$$

$$T_0=T_1 \tag{4.15}$$

$$|b|=|c| \tag{4.16}$$

$$b<0 \tag{4.17}$$

$$c>0 \tag{4.18}$$

related with the boundary conditions (Eqs. (4.2-4)), the behavior of T=f(x,t) shown in Figure 4.2 is obtained. On the other hand, the experimental data obtained for the surface profile of Linera is given in Figure 4.3. Comparison of Figures 4.2 and 4.3 shows a similarity between the two profiles.

Thus, with the suitable parameters (k_1 ,k_2, A_0) and the constants of boundary

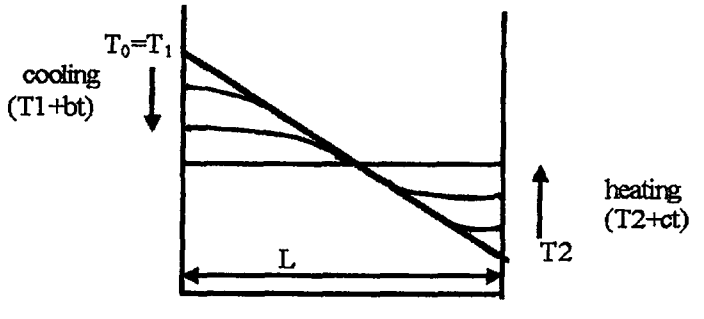

Figure 4.2 Sample Temperature Profile for Eq. (4.13)

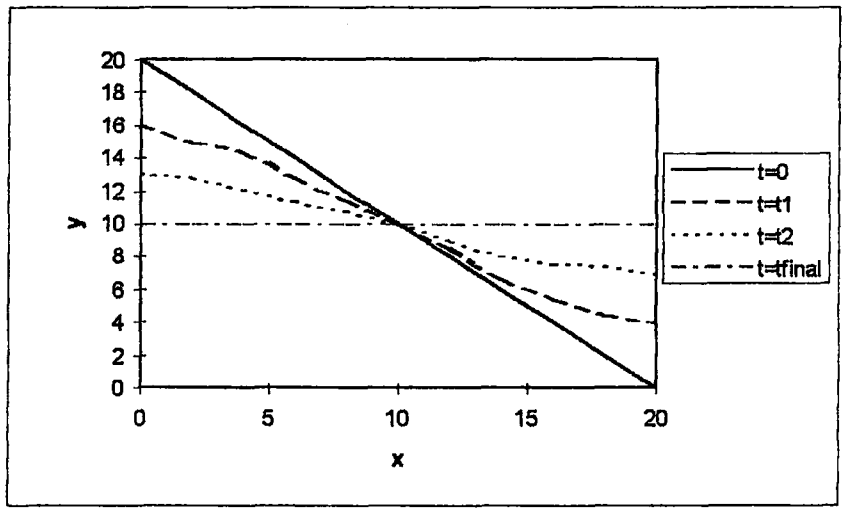

Figure 4.3 Sample Surface Profile of the flow of Linera

conditions (T_0, T_1, T_2, a, b, c), the surface profile of Linera can be modeled as analogous to the heat transport problem given in Section 4.1.1 provided that the constants in Eq. (4.13) are defined in terms of momentum transport. For analogy;

$$T \equiv y \tag{4.19}$$

Hence, by defining $k_3=A_0/k_2$, the model equation for the flow of Linera can be written as;

$$y=(y_1-y_0)\,\mathrm{erfc}\left(\frac{-x}{2\sqrt{k_1 t}}\right)$$

$$+(b-k_1k_3)\left[\left\{\left(t+\frac{(-x)^2}{2k_1}\right)\mathrm{erfc}\left(\frac{-x}{2\sqrt{k_1 t}}\right)\right\}-\left\{(-x)\left(\frac{t}{\pi k_1}\right)^{1/2}e^{-(-x)^2/(4k_1 t)}\right\}\right]$$

$$-(aL+y_0-y_2)\sum_{n=0}^{\infty}\mathrm{erfc}\left(\frac{-x+L(1+2n)}{2\sqrt{k_1 t}}\right)$$

$$-(k_1k_3-c)\sum_{n=0}^{\infty}\left[\left\{\left(t+\frac{(-x+L(1+2n))^2}{2k_1}\right)\operatorname{erfc}\left(\frac{-x+L(1+2n)}{2\sqrt{k_1t}}\right)\right\}-\left\{(-x+L(1+2n))\left(\frac{t}{\pi k_1}\right)^{1/2}e^{-(-x+L(1+2n))/(4k_1t)}\right\}\right]$$

$$-(y_1-y_0)\sum_{n=0}^{\infty}\operatorname{erfc}\left(\frac{-x+2nL}{2\sqrt{k_1t}}\right)$$

$$-(b-k_1k_3)\sum_{n=0}^{\infty}\left[\left\{\left(t+\frac{(-x+2nL)^2}{2k_1}\right)\operatorname{erfc}\left(\frac{-x+2nL}{2\sqrt{k_1t}}\right)\right\}-\left\{(-x+2nL)\left(\frac{t}{\pi k_1}\right)^{1/2}e^{-(-x+2nL)/(4k_1t)}\right\}\right]$$

$$+(aL+y_0-y_2)\sum_{n=0}^{\infty}\operatorname{erfc}\left(\frac{x+L(1+2n)}{2\sqrt{k_1t}}\right)$$

$$+(k_1k_3-c)\sum_{n=0}^{\infty}\left[\left\{\left(t+\frac{(x+L(1+2n))^2}{2k_1}\right)\operatorname{erfc}\left(\frac{x+L(1+2n)}{2\sqrt{k_1t}}\right)\right\}-\left\{(x+L(1+2n))\left(\frac{t}{\pi k_1}\right)^{1/2}e^{-(x+L(1+2n))/(4k_1t)}\right\}\right]$$

$$+(y_1-y_0)\sum_{n=0}^{\infty}\operatorname{erfc}\left(\frac{x+2nL}{2\sqrt{k_1t}}\right)+$$

$$+(b-k_1k_3)\sum_{n=0}^{\infty}\left[\left\{\left(t+\frac{(x+2nL)^2}{2k_1}\right)\operatorname{erfc}\left(\frac{x+2nL}{2\sqrt{k_1t}}\right)\right\}-\left\{(x+2nL)\left(\frac{t}{\pi k_1}\right)^{1/2}e^{-(x+2nL)/(4k_1t)}\right\}\right]$$

$$+\left[(k_1k_3)t\right]+ax+T_0 \qquad (4.20)$$

where y_0, y_1 and y_2 are initial positions in the container, L is the width of the container, a, b and c are constants of the boundary conditions (Figure 4.4), k_1 and k_3 are momentum transport parameters.

4.1.3 Wall Slip Correction

In the surface profile determination experiment, a little amount of Linera was left on the side surfaces of the glass container due to wall slip. Thus, a wall slip correction factor has to be added to Eq. (4.20). Experimental observations indicated a time-dependent correction factor due to the accelerated adhesion of Linera on the glass surfaces between the initial and final states and it was found that total height

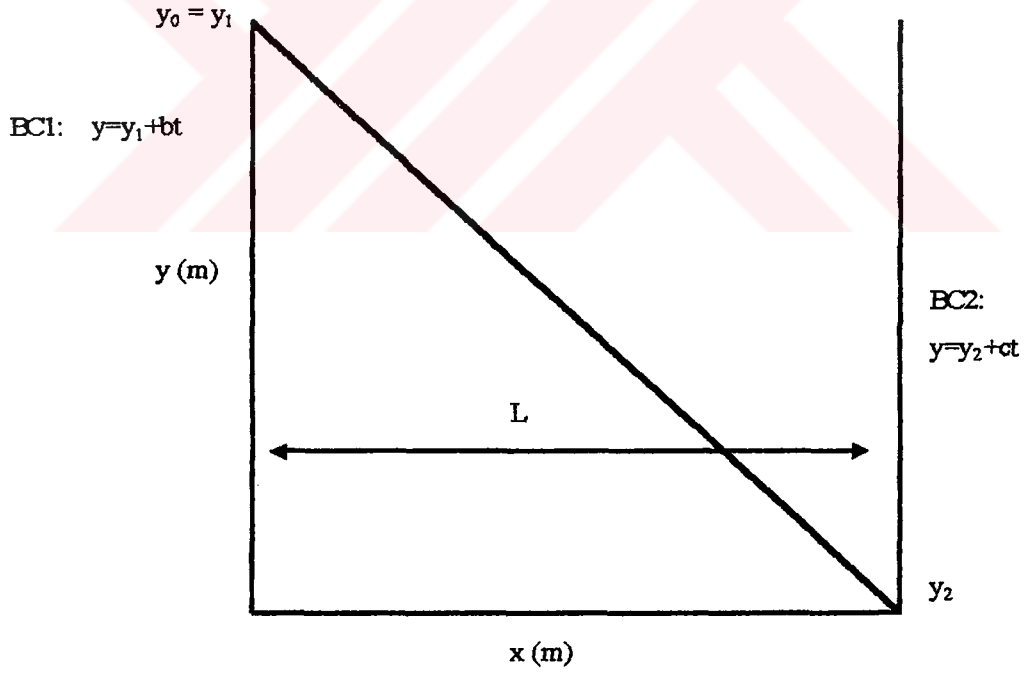

Figure 4.4 Schematic Diagram for the Surface Flow of Linera

loss in Linera was 0.002 m due to adhesion to glass walls (Figure 4.5). It was seen that the error function can model the adhesion to glass walls due to wall slip Linera. Therefore the following correction factor was added to Eq. (4.20)

$$-0.002\left(1-\operatorname{erfc}\left(\frac{3t}{\left(\frac{y_1+y_2}{2}-y_1\right)/b}\right)\right) \tag{4.21}$$

where t is the time at any instant, $\left(\frac{y_1+y_2}{2}-y_1\right)/b$ is the total time between initial and final states of flow and 0.002 is a parameter to convert error function of $\left(\frac{3t}{\left(\frac{y_1+y_2}{2}-y_1\right)/b}\right)$ to height loss of Linera. And the equation defining the surface flow of Linera is the summation of Eqs. (4.20) and (4.21) given as;

$$y = \text{Eq. (4.20)} + \text{Eq. (4.21)} \tag{4.22}$$

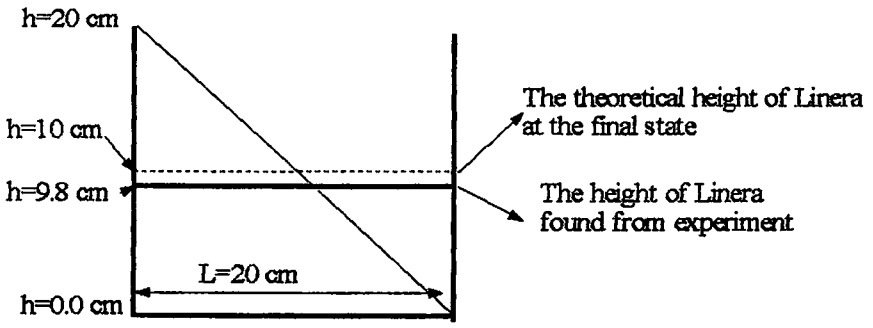

Figure 4.5 Schematic diagram of the container

4.1.4 Dimensional Analysis for the Momentum Transport Parameters (k1 and k3)

In the model equation for the surface flow of Linera (Eq. 4.22) adapted from 1-D heat transfer with generation, a position dependent initial condition and time dependent linear boundary conditions in a slab, the corresponding expressions for parameters, k_1 and k_3 for fluid mechanics have to be determined. Buckingham-Pi Method was used for this purpose. The variables and their dimensions involved in k_1 are;

k_1 = model parameter in Eq. (4.22) (L^2/θ)

ρ= fluid density (M/L^3)

μ= fluid viscosity $(M/(L\theta))$

g= acceleration (L/θ^2)

P= pressure $(M/(\theta^2 L)$

L= length of the container (L)

D= width of the container (L)

V= fluid average velocity in y direction = (L/θ)

By application of the Buckingham-Pi theorem (Appendix F), the following dimensionless groups were deduced.

$$\pi_1 = \left(\frac{\rho}{\mu}\right)k_1 \tag{4.23}$$

$$\pi_2 = \sqrt{\frac{\mu}{\rho V^5}}g \tag{4.24}$$

$$\pi_3 = \frac{P}{\rho V^2} \tag{4.25}$$

$$\pi_4 = \frac{LV\rho}{\mu} \tag{4.26}$$

$$\pi_5 = \frac{DV\rho}{\mu} \tag{4.27}$$

Thus the Buckingham-Pi theorem yields;

$$\pi_1 = K(\pi_2)^a(\pi_3)^b(\pi_4)^c(\pi_5)^d \tag{4.28}$$

where K, a, b, c and d are experimentally determined dimensionless constants, yielding

$$\frac{\rho}{\mu}k_1 = K\left(\sqrt{\frac{\mu}{\rho V^5 g}}\right)^a\left(\frac{P}{\rho V^2}\right)^b\left(\frac{\rho VL}{\mu}\right)^c\left(\frac{\rho VD}{\mu}\right)^d \tag{4.29}$$

or

$$k_1 = \frac{\mu}{\rho}K\left(\sqrt{\frac{\mu}{\rho V^5 g}}\right)^a\left(\frac{P}{\rho V^2}\right)^b\left(\frac{\rho VL}{\mu}\right)^c\left(\frac{\rho VD}{\mu}\right)^d \tag{4.30}$$

In the similar manner, k_3 (1/m) was analyzed and it was found as;

$$k_3 = \left(\frac{g}{\rho P}\right)K\left(\frac{\rho^{1/2}g\mu}{P^{3/2}}\right)^a\left(\frac{\rho gL}{P}\right)^b\left(\frac{\rho^{1/2}V}{P^{1/2}}\right)^c\left(\frac{\rho gD}{P}\right)^d \tag{4.31}$$

4.2 Determination of V_y from y(x,t)

The velocity profile of Linera can be determined from the surface profile (Eq. (4.22)). The use of these velocity profiles provides a further verification between the proposed deterministic model and the experimental data.

Definition of the instantaneous velocity is given as;

$$V_y = \frac{dy}{dt} \tag{4.32}$$

and y=f(x,t) is known (Eq. 4.22). So, V_y can be determined by taking the derivative of y with respect to time. Using Leibnitz Rule (Appendix D), the equation giving the velocity profile can be expressed as;

$$V_y = (y_1 - y_0)\left\{\frac{1}{\sqrt{\pi}} e^{-\left(\frac{-x}{2\sqrt{k_1 t}}\right)^2} \frac{-x}{2t\sqrt{k_1 t}}\right\}$$

$$+(b - k_3 k_1)\left\{\operatorname{erfc}\left(\frac{-x}{2\sqrt{k_1 t}}\right) + \left[\left(t + \frac{(-x)^2}{2k_1}\right)\left(\frac{1}{\sqrt{\pi}} e^{-\left(\frac{-x}{2\sqrt{k_1 t}}\right)^2} \frac{(-x)}{2t\sqrt{k_1 t}}\right)\right]\right.$$

$$\left. - e^{-(-x)^2/(4k_1 t)}\left[\frac{(-x)}{2(\pi k_1 t)^{1/2}} + (-x)^3\left(\frac{t}{\pi k_1}\right)^{1/2} \frac{1}{4t^2 k_1}\right]\right\}$$

$$-(aL + y_0 - y_2)\sum_{n=0}^{\infty}\left\{\frac{1}{\sqrt{\pi}} e^{-\left(\frac{-x+L(1+2n)}{2\sqrt{k_1 t}}\right)^2} \frac{-x + L(1+2n)}{2t\sqrt{k_1 t}}\right\} -$$

$$-(k_3 k_1 - c)\sum_{n=0}^{\infty}\left\{\operatorname{erfc}\left(\frac{-x + L(1+2n)}{2\sqrt{k_1 t}}\right) + \left[\left(t + \frac{(-x + L(1+2n))^2}{2k_1}\right)\right.\right.$$

$$\left.\left.\left(\frac{1}{\sqrt{\pi}} e^{-\left(\frac{-x+L(1+2n)}{2\sqrt{k_1 t}}\right)^2} \frac{(-x + L(1+2n))}{2t\sqrt{k_1 t}}\right)\right]$$

$$- e^{-(-x+L(1+2n))^2/(4k_1 t)}\left[\frac{-x + L(1+2n)}{2(\pi k_1 t)^{1/2}} + \right.$$

$$\left.\left. (-x + L(1+2n))^3\left(\frac{t}{\pi k_1}\right)^{1/2} \frac{1}{4t^2 k_1}\right]\right\} -$$

$$-(y_1-y_0)\sum_{n=0}^{\infty}\left\{\frac{1}{\sqrt{\pi}}e^{-\left(\frac{-x+2nL}{2\sqrt{k_1t}}\right)^2}\frac{-x+2nL}{2t\sqrt{k_1t}}\right\}-$$

$$-(b-k_3k_1)\sum_{n=0}^{\infty}\left\{\operatorname{erfc}\left(\frac{-x+2nL}{2\sqrt{k_1t}}\right)+\left[\left(t+\frac{(-x+2nL)^2}{2k_1}\right)\left(\frac{1}{\sqrt{\pi}}e^{-\left(\frac{-x+2nL}{2\sqrt{k_1t}}\right)^2}\frac{(-x+2nL)}{2t\sqrt{k_1t}}\right)\right]\right.$$

$$\left.-e^{-(-x+2nL)^2/(4k_1t)}\left[\frac{-x+2nL}{2(\pi k_1t)^{1/2}}+(-x+2nL)^3\left(\frac{t}{\pi k_1}\right)^{1/2}\frac{1}{4t^2k_1}\right]\right\}$$

$$+(aL+y_0-y_2)\sum_{n=0}^{\infty}\left\{\frac{1}{\sqrt{\pi}}e^{-\left(\frac{x+L(1+2n)}{2\sqrt{k_1t}}\right)^2}\frac{x+L(1+2n)}{2t\sqrt{k_1t}}\right\}$$

$$+(k_3k_1-c)\sum_{n=0}^{\infty}\left\{\operatorname{erfc}\left(\frac{x+L(1+2n)}{2\sqrt{k_1t}}\right)+\left[\left(t+\frac{(x+L(1+2n))^2}{2k_1}\right)\left(\frac{1}{\sqrt{\pi}}e^{-\left(\frac{x+L(1+2n)}{2\sqrt{k_1t}}\right)^2}\frac{(x+L(1+2n))}{2t\sqrt{k_1t}}\right)\right]\right.$$

$$\left.-e^{-(x+L(1+2n))^2/(4k_1t)}\left[\frac{x+L(1+2n)}{2(\pi k_1t)^{1/2}}+(x+L(1+2n))^3\left(\frac{t}{\pi k_1}\right)^{1/2}\frac{1}{4t^2k_1}\right]\right\}$$

$$+(y_1-y_0)\sum_{n=0}^{\infty}\left\{\frac{1}{\sqrt{\pi}}e^{-\left(\frac{x+2nL}{2\sqrt{k_1t}}\right)^2}\frac{x+2nL}{2t\sqrt{k_1t}}\right\}+$$

$$+(b-k_3k_1)\sum_{n=0}^{\infty}\left\{\operatorname{erfc}\left(\frac{x+2nL}{2\sqrt{k_1t}}\right)+\left[\left(t+\frac{(x+2nL)^2}{2k_1}\right)\left(\frac{1}{\sqrt{\pi}}e^{-\left(\frac{x+2nL}{2\sqrt{k_1t}}\right)^2}\frac{(x+2nL)}{2t\sqrt{k_1t}}\right)\right]\right.$$

$$\left.-e^{-(x+2nL)^2/(4k_1t)}\left[\frac{x+2nL}{2(\pi k_1t)^{1/2}}+\frac{(x+2nL)^3}{}\left(\frac{t}{\pi k_1}\right)^{1/2}\frac{1}{4t^2k_1}\right]\right\}$$

$$+(k_3k_1)$$

$$-0.002\left[e^{-\left(\frac{3t}{\left(\frac{y_1+y_2}{2}-y_1\right)/b}\right)^2}\frac{6}{\sqrt{\pi}}\frac{1}{\left(\frac{y_1+y_2}{2}-y_1\right)/b}\right] \qquad (4.33)$$

4.3 Parameter Evaluation using the Modified Simplex Method

The parameters (k1, k3, b and c) in Eq. (4.22) has to be evaluated by an optimization technique so as to obtain their characteristic values which fit the experimental data. For this purpose, the Modified simplex method of Nelder and Mead (1965) was used.

The computer program developed for this purpose consists of two parts; optimization and the evaluation of the proposed model (Eq. (4.22)). The algorithm of the computer program is given in Figure 4.6. The program was written in the FORTRAN Programming Language by the help of 'Microsoft FORTRAN

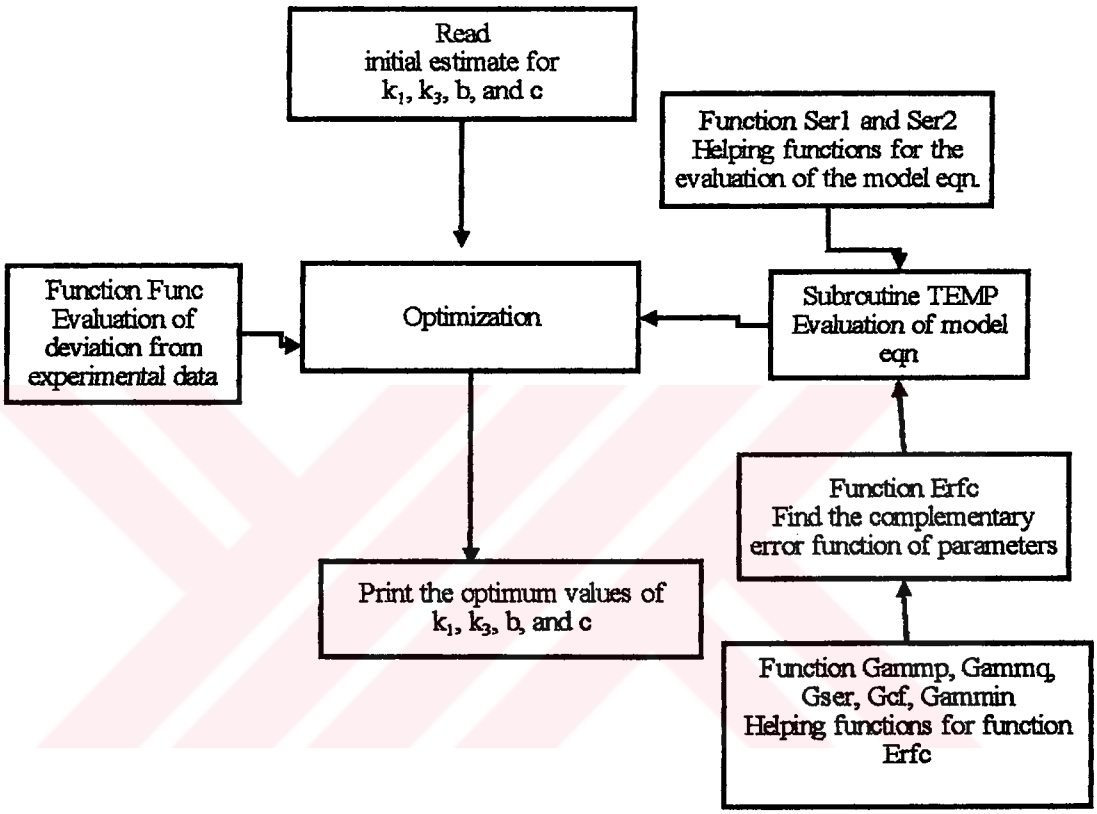

Figure 4.6 The Logic Diagram of the Computer Program for Parameter Evaluation

Workbench 1.0' (compiler). The subroutines that are related with the evaluation of erf(x) was taken from 'Numerical Recipes Software in FORTRAN'. The program was run on an IBM compatible computer (486 DX-4 processor, 8 MB RAM, 850 MB hard disk) and the values of the parameters were obtained as;

$$k_1 = 1.87\ E\text{-}5\ \ (m^2/s) \tag{4.34}$$

$$k_3 = -1.99E\text{-}3\ \ (m^{-1}) \tag{4.35}$$

$$b = -0.000143\ (m/s) \tag{4.36}$$

$$c = 0.000143\ (m/s) \tag{4.37}$$

CHAPTER 5

RESULTS AND DISCUSSION

In the present study, it was aimed to simulate the transient surface profiles of Linera by means of a deterministic model and to relate surface flow of Linera to its spreadability. Although there is numerical solution to this kind of free surface flow problem, an analytical solution was preferred because of its easy adaptation to the system under consideration (Chapter 2, Section 2.5.1). The Equation describing the surface flow of Linera was adapted from heat transfer (Chapter 4, Section 4.1). The corresponding momentum transport parameters were derived and their physical meaning were explained through dimensional analysis (Chapter 4, Section 4.1.4) and their numerical values were determined using optimization techniques (Chapter 4, Section 4.3).

5.1 Physical Properties of Linera

Density and flow behavior of Linera were the experimental parameters which needed to be determined to explain the physical meaning of the momentum transport parameters in the equation giving the surface flow of Linera (Eq. 4.22).

The bulk density of Linera was found as 974.7 kg/m^3 (Chapter 3, Section 3.2.1.1). The major ingredients of cream cheese products are milk-fat and moisture. The density of milk-fat is 915 kg/m^3 (Roy et al.,1971) and that of water is 1000 kg/m^3. The density measurement showed that Linera is a type of cream cheese with relatively high moisture content. This is an expected result since Linera is marketed as a diet food product.

In the present study, the flow behavior of Linera was simulated by using the Herschel-Bulkley model given by Eq. (2.10). Figure 5.1 shows the relationship between apparent viscosity and shear stress of Linera. The fact that apparent viscosity tends to a constant value shows Linera experiences no yield stress at 20 ^{0}C.

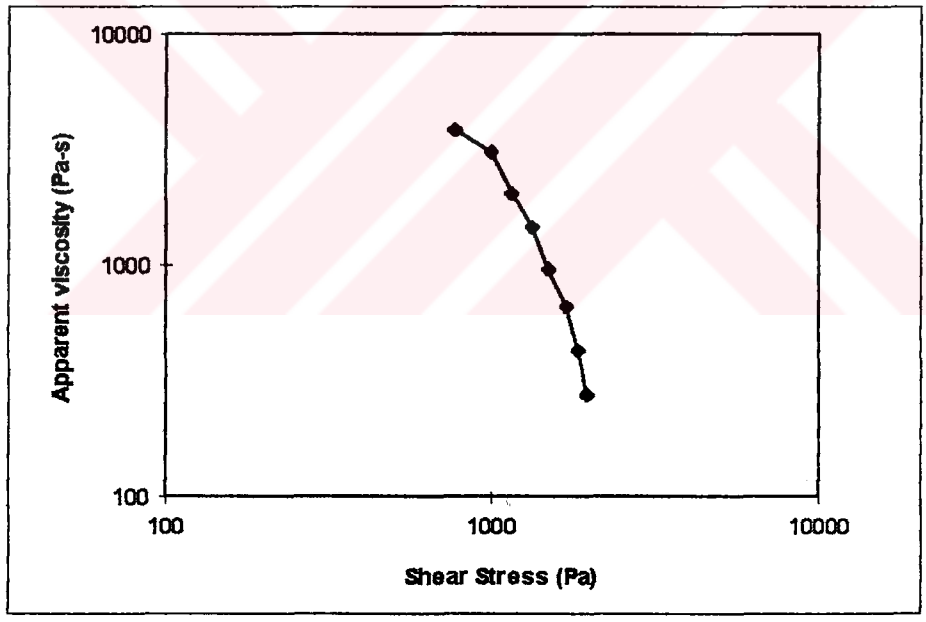

Figure 5.1 Logarithmic relationship between apparent viscosity and shear stress of Linera at 20 ^{0}C

Thus the Herschel-Bulkley model for Linera reduces to the power law model (Eq. (2.9)) where K=1288 Pa-s^n and n=0.25 as described in Appendix A, Section A.2. Figure 5.2 shows when shear rate increases, the apparent viscosity decreases and that indicates Linera is a shear-thinning liquid.

In the literature, Soft cheeses (such as cream cheese) are usually considered as thixotropic materials due to their viscoelastic properties (Chapter 2, Section 2.3). The viscoelastic properties are related with the solid content of cream cheese. When the amount of solid content (milk-fat) decreases, the viscoelastic properties decrease and the flow reduces to a shear-thinning flow (Jao et al., 1981). The moisture content is a factor which contributes to the flowability and spreadability of the creamed product. A high moisture content means a large volume of the aqueous phase with protein particles and fat globules packed not as densely as in low-moisture product.

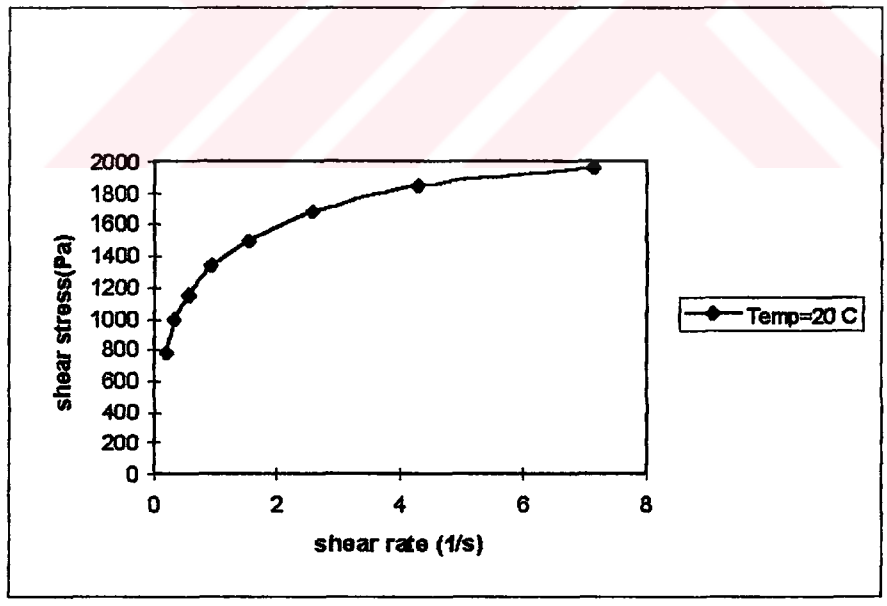

Figure 5.2 Shear stress-Shear rate relationship of Linera at 20 ^{0}C

This facilitates the mobility of the corpuscular constituents during spreading (Kalab and Modler, 1985). Linera being a diet food product has a low milk-fat content and high moisture content resulting in higher flowability and spreadability which can be modelled as a shear-thinning liquid with high spreadability due to no yield stress.

5.2 Comparison and Interpretation of Experimental and Theoretical Results of Transient Surface Profiles of Linera

Bu using the optimization program for data fitting (Chapter 4, Section 4.3), the following parameters for the model equation (Eq. 4.22)

$$k_1=1.87\ E\text{-}5\ \ (m^2/s) \tag{5.1}$$

$$k_3=-1.99E\text{-}3\ \ (m^{-1}) \tag{5.2}$$

$$b=-0.000143\ (m/s) \tag{5.3}$$

$$c=0.000143\ (m/s) \tag{5.4}$$

were obtained and the theoretical surface profile and velocity profile of Linera were found using these parameters. Figure 5.3, comparing the theoretical and experimental surface profiles at different instants of time, shows that there are position differences in y direction between experimental and theoretical surface profiles, especially at the start of motion (t=150 sec). At the start of motion, there is a very fast change in the y direction of experimental surface profiles due to the high static pressure difference ($P=\rho gh$). Thus linear time dependent boundary conditions seem to be an oversimplification at the beginning of flow, since wall slip has been accounted for in the theoretical approach by introducing a correction factor (Chapter 4, Section 4.1.3). This also causes a discrepency between the theoretical and

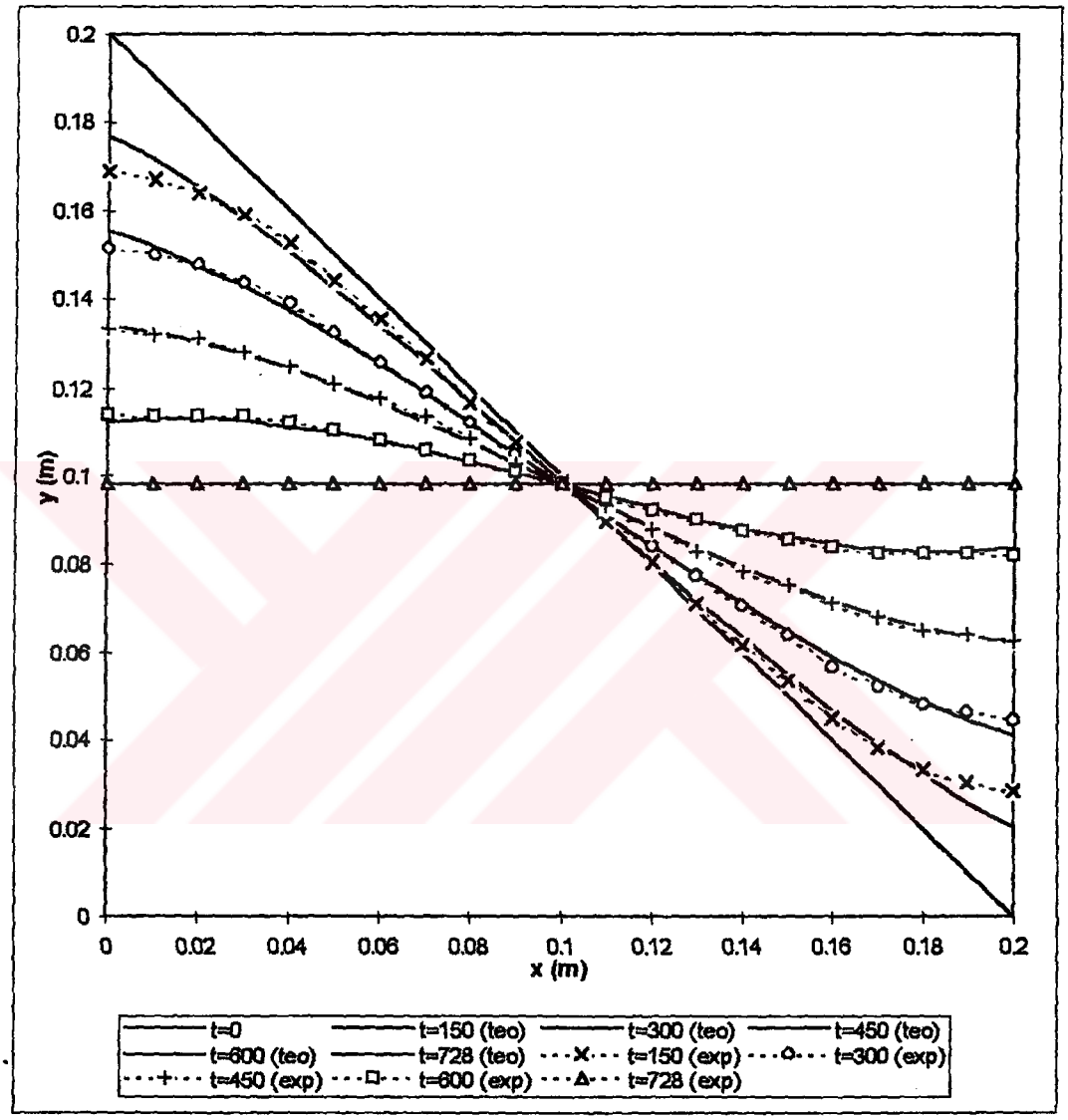

Figure 5.3 The Transient Surface Profiles of Linera

experimental velocity profiles given in Figure 5.4 .

The slopes of the curves in Figure 5.3 can further be used to find the relative spreadability of viscoelastic materials with negligibly low yield stress where higher slopes indicate better spreadability.

5.3 Dimensional Analysis and Interpretation of the Momentum Transport Parameters of the Model Equation

By using the Buckingham Pi Method for dimensional analysis (Chapter 4, Section 4.1.4), k_1 is found to be a function of the following parameters;

$$k_1 = K\frac{\mu}{\rho}\left(\sqrt{\frac{\mu}{\rho V^5}g}\right)^a\left(\frac{Pr}{\rho V^2}\right)^b\left(\frac{\rho VL}{\mu}\right)^c\left(\frac{\rho VD}{\mu}\right)^d \qquad (5.5)$$

where $\frac{\mu}{\rho}$ is the momentum diffusivity, $\left(\sqrt{\frac{\mu}{\rho V^5}g}\right)$ is a dimensionless number which relates the viscous and gravitational forces during flow, $\frac{Pr}{\rho V^2}$ is the Euler number and $\frac{\rho VD}{\mu}$ or $\frac{\rho VL}{\mu}$ are Reynolds numbers based on the length and the width of the container. Thus Eq. (5.5) can be written as

$$k_1 = K\frac{\mu}{\rho}\left(\sqrt{\frac{\mu}{\rho V^5}g}\right)^a\left(N_{Euler}\right)^b\left(N_{Reynolds_1}\right)^c\left(N_{Reynolds_2}\right)^d \qquad (5.6)$$

where K, a, b, c, and d are constants.

In the similar manner, k_3 was analyzed (Chapter 4, Section 4.1.4) and it was found as;

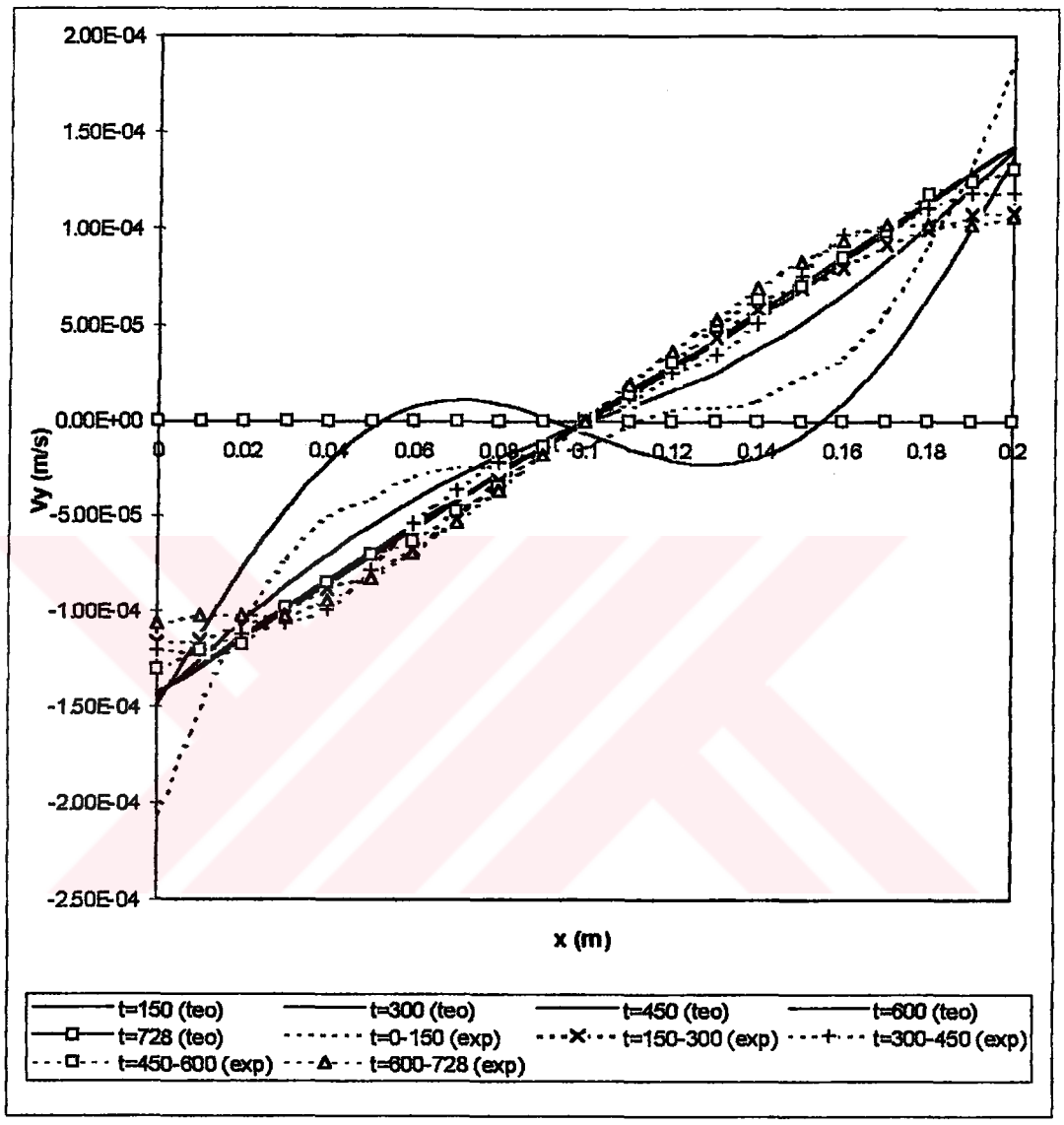

Figure 5.4 Velocity Profiles of Linera

$$k_3 = K\left(\frac{g}{\rho Pr}\right)\left(\frac{\rho^{1/2} g\mu}{Pr^{3/2}}\right)^a\left(\frac{\rho gL}{Pr}\right)^b\left(\frac{\rho^{1/2} V}{Pr^{1/2}}\right)^c\left(\frac{\rho gD}{Pr}\right)^d \quad (5.7)$$

or the combination of $\left(\frac{\rho gL}{Pr}\right)$ and $\left(\frac{\rho^{1/2} V}{Pr^{1/2}}\right)$ gives

$$k_3 = K\left(\frac{g}{\rho Pr}\right)\left(\frac{\rho^{1/2} g\mu}{Pr^{3/2}}\right)^a\left(\frac{\rho gD}{Pr}\right)^d\left(\frac{V^2}{Lg}\right)^e \quad (5.8)$$

where $\left(\frac{g}{\rho Pr}\right)$ is a dimensional constant related with momentum generation parameters, $\left(\frac{\rho^{1/2} g\mu}{Pr^{3/2}}\right)$ and $\left(\frac{\rho gD}{Pr}\right)$ are dimensionless numbers which are related with the complex interaction of gravitational and pressure forces, and $\frac{V^2}{Lg}$ is the Froude number which especially comes into prominence in flow with free surface.

The majority of the dimensionless number obtained from the anlaysis for momentum transport parameters are related with momentum generation (gravitational force or pressure effect), as seen in Euler number (the ratio of inertial to gravitational forces), in Froude number (the ratio of inertial to gravitational forces) and in other complex dimensionless numbers specific to the free surface flow

CHAPTER 6

CONCLUSIONS AND FUTURE WORK

6.1 Conclusions

It was seen that the free surface flow of the high moisture content cream cheese, Linera, can be simulated by means of an analogy to the deterministic heat transfer model for 1-D heat conduction in a slap with constant generation rate together with a linear position-dependent initial condition and time-dependent boundary conditions which can further be used to evaluate relative spreadabilities of viscoelastic materials exhibiting negligibly low yield stresses.

The model suggested falls short for the prediction of the transient flow profiles especially at the initial stages of flow suggesting that the relationship between time and the boundary conditions are more complex than linear.

Dimensionless analysis proved that the model parameters of the momentum transport problem are related with the momentum generation rate revealing interrelationships between gravitational, pressure and inertial effects.

6.2 Future Work

The discrepancy between the experimental and theoretical transient free surface profiles during the initial stages of flow can be overcome by the use of higher order polynomial or error functional dependencies between time and the boundary conditions.

Relative spreadabilities of viscoelastic materials with negligible yield stress can be evaluated by taking sets of data on a variety of such materials.

REFERENCES

Bagley, E. B., 1957. ' End Correction in the Capillary Flow of Polyethylene', J. Appl Physics, vol 28, p 624.

Bagley, E. B., Christianson, D.D. ,1982. 'Smelling Capacity of Starch and Its Relationship to Suspension Viscosity', J. Texture Studies., vol. 13, p 115-126.

Balmecada, E., Huang, F. and Rha, C.K., 1973. 'Rheological Properties of Hydrocolloids'. J. Food Sci., vol 38 p 1169.

Barbosa, G.V. and Peleg, M. ,1983. 'Flow parameters of Selected Commercial Semi-Liquid Food Products', J. Texture Studies, vol 3, p 69.

Brodkey R.S., 1967. 'The Phenomena of Fluid Motion', Addison Reading, Massacuhettes.

Campanella, O. H. and Peleg, M. ,1987. 'Determination of the Yield Stress of Semi-Liquid Foods from Squeezing Flow Data', J. Food Sci., vol. 52, p 214.

Casson, N ,1959 . 'A Flow Equation for Pigmented-oil Suspension of the Printing ink type'. In Rheology of Disperse Systyems, Pergamon Press, Newyork.

Charm, S.E.,1963. 'The Direct Determination of Shear Stress-Shear Rate Behavior of Foods in the Presence of a Yield Stress'. J. Food Sci. vol 28 p 107-113.

Davis, S. S. ,1973. 'Rheological Properties of Semi-solid Foodstuff', J. Texture Study. , vol. 4, p 15-40.

Dickie, A. and Kokini, J.L., 1982. 'A Model of Food Spreadability from Fluid Mechanics, J. Texture Studies, vol 13, p 211.

Dixon, B.D. and Parekh, J.V., 1977. ' The use of a Cone Penetrometer to Measure Spreadability of Butter or Dairy Blend', Dairy Technology, vol 8, p 15.

Desrosier, W., 1977. Elements of Food Technology, Avi Publishing Company, Connecticut.

Dutta B. and Sastry S., 1990. 'Velocity Distribution of Food Particle Suspension in Holding Tube Flow: Experimental and Modelling Studies on Average Particle Velocities', Journal of Food Science, vol. 55, p 1448-1453.

Figoni, P. I. and Shoemaker, C. R. ,1983. 'Characterization of Time-Depentent Flow Properties of Mayonnaise under Steady Shear', J. Texture Studies, vol.14, p 431-442.

Fletcher, R. ,1991. Practical Methods of Optimization, 2nd Edition, John Wiley and Sons, New York.

Geankoplis, C.J., 1983. 'Transport Process and Unit Operations, 2nd Edition, Allyn and Bacon Inc., Boston.

Gencer, G. and Peleg, M., 1984. 'Digitizer Aided Determination of Yield Stress in Semi-Liquid Foods, J. Food Sci, vol 49, p 1620.

Hahn, S.J , Ree, T. and Eyring H, 1959. 'Flow mechanisms of thixotropic substances', Int. Eng. Chem, vol 51 p856-857.

Hansen, E. B. and Kelmanson, M. A. ,1994. 'Steady, Viscous, Free Surface Flow on a Rotating Cylinder', J. of Fluid Mechanics, vol. 272, p 91-107.

Heldman, D. R. and Lund, D. B. ,1992. Handbook of Food Engineering, 1st Edition, Marcel Decker Inc., New York.

Higgs, S. J. and Norrington, R. J. ,1971. 'Rheological Properties of Selected Food Stuff', Proc. Biochem., vol 6, p 52-54.

Jao, Y.C., Chan, R.V. and Chaudhari, R.V, 1981. 'Rheology of Enzyme Modified Cheese', J. Food Sci., vol 46, p 254.

Kalab, M. and Modler, H.W., 1985. 'Milk Gel Structure; Electron Microscopy of Whey Protein-Based Cream Cheese Spread', Milchwissenchaft, vol 40, p 193-196.

Kalab, M. and Modler, H.W., 1985b.'Development of Microstructure in a Cream Cheese Based on Queso Blanco Cheese, Food Microstructure, vol 4 p 89.

Kokini, J. L. and Dickie, A. ,1981. 'An Attempt to Identfy and Model Transient Viscoelastic Flow in Foods', J. of Texture Studies., vol. 13, p 539-557.

Kokini, J. L. and Dickie A. ,1982. 'A Model of Food Spreadability from Fluid Mechanics', J. of Texture Studies., vol. 13, p 211-227.

Konstance, R.P. and Holsinger V.H., 1992. 'Development of Rheological Test Methods for Cheese' , Food Tech, Iss 1, p 105.

Kothe, D. B. and Mjolsness, R. C. ,1992. 'RIPPLE: A new Model Incompressible Flows with Free Surface', AIAA Journal, vol. 30, p 2694-2700.

Lusisano, M., Casiraghi, E. and Pompei C., 1989. ' Optimization of an instrumental method for the evaluation of spreadability', J. Texture Studies, vol 20, p301.

Mason, P. L., Bistany, K. L. and Puoti, M ,1982. ' A new Model to Simulate Transient Shear Stess Growth in Semi Solid Foods', J. Food Process Engineering, vol 1, p 219-233.

Massaguer-Roig, S, Rizvi, S. H. and Kosinowski, F. V., 1984. 'Characterization of Thixotropic Behavior of Soft Cheeses', J. Food Sci, vol 49, p 668.

Meer, J. J. and Fryer, P. J. ,1992. 'A Model for Fluid Flow and Mixing in a Cavity Transfer Mixer', Food and Bioproducts Processing, vol. 70, p 183-192.

Mewis, J., 1980. 'Rheology of Suspension'. Rheology vol 1 ,Plenum Press, Newyork.

Mills, PL and Kokini, JL, 1984. 'Comparison of steady shear and dynamic viscoelastic properties of guar and karaya gums'. J. Food Sci., vol 49 p1.

Mizrahi, S and Berk, Z. ,1972. 'Flow Behavior of Concentrated Orange Juice'. J. Texture Studies vol 3 p 69-79.

Mortensen, B. K and Danmark, H., 1982. 'Consistency Characteristic of Butter', Milchwissenschaft, vol 37, p 530.

Moskowitz, H. W., 1987. 'Food Texture', Marcel Dekker Inc, Boston.

Nakayama, T., Niwo, E. and Homada, I ,1980. 'Pipe Transportation of Minced Fish Paste' J. Food Sci, vol 45 p 844-847.

Nelder, J. A. and Mead, R ,1965. 'A Simplex Method for Function Minimization', Computer J. vol 7 p 308-313.

Nolan, E. J. and Holsinger, U. H. ,1989. 'Dynamic Rheological Properties of Natural and Imitation Mozzarella Cheese', J. of Texture Studies., vol. 20, p 179-189.

Osorio, F. A. and Steffe, J. F. ,1984. 'Kinetic Energy Calculations for Non-Newtonian Fluids in Circular Tubes', J. of Food Science, vol. 49, p 1295-1296.

Prentice, J.H 1972. 'Rheology and Texture of Dairy Products'. J. Texture Studies, vol 3, p 415.

Pryce-Jones, J. ,1953. 'The Rheology of Honey', J. Texture Sdudies, vol. 3, p 415-458.

Rao, M. A. ,1977a. Rheology of Liquid Foods, J. Texture Study. , vol. 8, p 135-168.

Rao, M. A , 1977b. 'Measurement of Flow Properties of Fluid Foods'. J. Texture Studies vol 8 p 257-282.

Rao,M. A., Bourne, M. C. and Cooley, H. S., 1981. 'Flow Properties of Tomato Concentrates', J. Texture Studies, vol 12 p521-538.

Rao, M. A. and Cooley, H. J., 1983. 'Applicability of Models with Yield for Tomato Concentrates', J. Food Process Engr., vol 6 p159-173.

Rao, M. A. and Rizvi A., 1986. 'Engineering Properties of Food', Marcel Dekker Inc., Newyork.

Roy, N. K., Yadav, P. L. and Dixit, R., 1971. 'Density of Buffalo Milk Fat'. Milchwissenschaft vol 26 p 735-738.

Schaller, A. and Knorr, D. ,1973. 'Ergebnisse methodolischer untersuchungen zur schatzung der fliessgrenze und plastischen viscositat am beispiel von apprikosenpuree unter zugrundelegung lines idealplastischen fliessverhaltens'. Confructa vol 18 p 169-176.

Spendley, W., Himsure, F. R. and Hext, GR,1962. 'Sequential Application of Simplex Designs in Optimization'. Technometrics, vol 4 p441-461.

Steath, B. B. ,1976. 'Viscosity Measurements and Interpretation of Viscosity Data', J. Texture Study. , vol. 7, p 157.

Strohmaier, W., Klostermeyer, H. and Devritz, H., 1992. 'Comparison of Different Methods to Determine the Spreadability and Firmness of Processed Cheese', Zeitschnift fur Lebensmittel-Untersuchung und Forschung, vol 194, p 531.

Tanner, R. I. ,1985. Enginnering Rheology, 1st Edition, Clarendon Press, Oxford.

Tiu, C. and Boger, D. V., 1974. 'Complete Rheological Characterization of time-dependent products', J. Texture Studies, vol 5, p 329.

Tung, M. A., Richards, J. F. and Morrison, B. C., 1970. 'Rheology of Fresh Egg White', J. Food Science, vol. 35, p 872-874.

Van Wazer, J. R.. , Lyons, J. W. and Kim, K. Y , 1963. 'Viscosity and flow measurement', Interscience, Newyork.

Vetterling, W.T, Teukolsky, S. A., Press, W. H. and Flannery, B. P. ,1985. Numerical Recipes Example Book, !st Edition, Cambridge University Press, Cambridge.

Vitali, A. A. and Rao, M. A., 1982. 'Flow Behavior of Guvaa Puree as a Function of Temperature and Concentration', J. Texture Studies, vol 13, p 275-289.

Vitali, A. A and Rao, M. A., 1984. 'Flow properties of low-pulp concentrated orange juice'. J. Food Sci. vol 49 p 876-881.

Weltman, R. N., 1943. 'Breakdown of thixotropic structure as function of time'. J. Appl. Physics, vol 14, p343.

Walters, K. ,1975. Rheometry, 1st Edition, Chapman and Hall, London
White, G. W. ,1970. Rheology in Food Research, J. Food Technol. , vol. 5 p 1-32.

Wharlow, R. W. ,1980. Rheological Techniques, 1st Edition, John Wiley and Sons, New York.

White, G. W. ,1970. 'Rheology in Food Research'. J. Food Technol. vol 5 p 1-32.

APPENDIX A

STEADY SHEAR RHEOLOGICAL BEHAVIOR OF LINERA

A.1 Calculation of the Apparent Viscosity

The calculation factors for the rheometer are

$$A\ (Pa / \tau\ \%) = 70 \qquad (A.1)$$

$$M\ (s^{-1} / \dot{\gamma}\ \%) = 2.0/\Delta h \qquad (A.2)$$

where A is the viscometer constant for shear stress, M is the viscometer constant for shear rate and Δh is the gap width in millimeters (1 mm). The data taken were multiplied by a correction factor of 70 (Pa / τ %) for the shear stress and 2.0 (s^{-1} / $\dot{\gamma}$ %) for the shear rate. Then the apparent viscosity was calculated as

$$\eta_a = \tau / \dot{\gamma} \qquad (A.3)$$

The the results are tabulated in Table (A.1).

A.2 Simulation of Steady Shear Rheological Data

The Herschel-Bulkley model was used to describe the flow behavior of

Table A.1 The Rheological Results of Linera at 20 ^{0}C

γ (%)	τ (%)	γ (s^{-1})	τ (Pa)	η_a (Pa-s)
0.1	11.1	0.2	777	3885
0.16	14.2	0.32	994	3106.25
0.28	16.4	0.56	1148	2050
0.46	19.1	0.92	1337	1453.26
0.77	21.3	1.54	1491	968.18
1.29	24.1	2.58	1687	653.88
2.15	26.3	4.3	1841	428.14
3.28	28.0	7.16	1960	273.74
5.99	-	11.98	-	-
10.00	-	20.00	-	-

Linera, given as;

$$\tau = \tau_0 + K(\dot{\gamma})^n \tag{A.4}$$

where K is the consistency index, n is the flow behavior index and τ_0 is the yield stress. It was found that Linera exhibited no yield stress (Chapter 5, Section 5.1). Thus, the model equation (Eq. (A.4)) reduces to the power law model;

$$\tau = K(\dot{\gamma})^n \tag{A.5}$$

or in logarithmic form;

$$\log \tau = n \log \dot{\gamma} + \log K \tag{A.6}$$

Log-log representation of shear stress vs. shear rate data (Figure A.1) was subjected to linear regression analysis yielding

$$\log \tau = 0.25 \log \dot{\gamma} + 3.11 \tag{A.7}$$

with an R^2 of 0.9836. Thus, the flow behavior index is

$$n=0.25 \tag{A.8}$$

and the consistency index is

$$K = \log^{-1}(3.11) = 1288.25 \ (Pa - s^n) \tag{A.9}$$

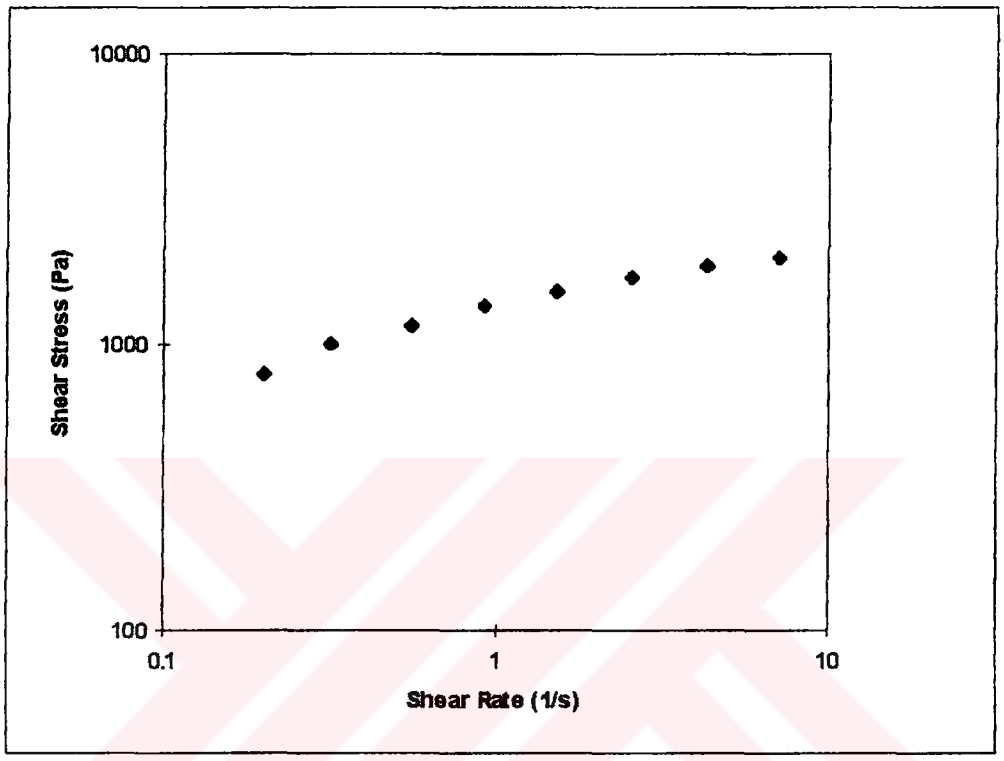

Figure A.1 Shear Rate versus Shear Stress Relationship of Linera at 20 ^{0}C

APPENDIX B

FUNDAMENTAL PROPERTIES OF LAPLACE TRANSFORMATION

Let V_1 and V_2 be functions whose Laplace transforms exits. Then

Theorem 1 : $L\{V_1 + V_2\} = L\{V_1\} + L\{V_2\}$ B.1

Theorem 2: $L\left\{\frac{\partial V}{\partial t}\right\} = pL\{V\} - V_0$ B.2

where V_0 is the value of $\lim_{t \to 0^+} V$. (i.e., V_0 is the initial condition)

Theorem 3: $L\left\{\frac{\partial^n V}{\partial x^n}\right\} = \frac{\partial^n \overline{V}}{\partial x^n}$ B.3

APPENDIX C

TABLE OF LAPLACE TRANSFORMS

$$\bar{v}(p) = \int_0^\infty e^{-pt} v(t)\, dt$$

and $q = \sqrt{\frac{p}{k}}$. k and x are always real and positive.

Table C.1 Table of Laplace Transformers

	$\bar{v}(p)$	v(t)
1.	$\frac{1}{p}$	1
2.	$\frac{1}{p^2}$	t
3.	e^{-qx}	$\frac{x}{2\sqrt{\pi k_1 t^3}} e^{-x^2/(4k_1 t)}$
4.	$\frac{e^{-qx}}{p^2}$	$\left(t+\frac{x^2}{2k_1}\right)\text{erfc}\left(\frac{x}{2\sqrt{k_1 t}}\right) - x\left(\frac{t}{\pi k_1}\right)^{1/2} e^{-x^2/(4k_1 t)}$
5.	$\frac{e^{-qx}}{p}$	$\text{erfc}\left(\frac{x}{2\sqrt{k_1 t}}\right)$

APPENDIX D

BINOMIAL THEOREM

If n is a positive integer,

$$(a+b)^n = \sum_{j=0}^{n} \binom{n}{j} a^{n-1} b^j$$

where $\binom{n}{j} = \frac{n!}{j!(n-j)!}$

Example:

$$\frac{1}{(1+z)^m} = (1+z)^{-m} = \sum_{n=0}^{\infty} \binom{-m}{n} z^n$$

APPENDIX E

LEIBNITZ'S RULE FOR DIFFERENTIATION OF INTEGRALS INVOLVING A PARAMETER

Rather frequently it is necessary to deal with a function $\varnothing$ (x) by the integral of the form

$$\varnothing(x) = \int_{A(x)}^{B(x)} f(x,t)\,dt \qquad t: \text{dummy variable.} \tag{E.1}$$

where f is such that the integration can not be effected analytically. In particular an expression for the derivative $\frac{d\varnothing}{dx}$ is often required.

$$\frac{d}{dx}\int_{A(x)}^{B(x)} f(x,t)\,dt = \int_{A(x)}^{B(x)} \frac{\partial f(x,t)}{\partial x}dt + f(x,B)\frac{dB}{dx} - f(x,A)\frac{dA}{dx} \tag{E.2}$$

which is valid for all values of x in the interval (a,b) when f and $\frac{\partial f}{\partial x}$ are continuous for $a \le x \le b$ and $A \le t \le B$ and when A'(x) and B'(x) are continuous in (a,b).

Note: $\operatorname{erf}(x) = \frac{2}{\sqrt{\pi}}\int_0^{\infty} e^{-z^2}\,dz$ z: dummy argument

APPENDIX F

APPLICATION OF THE BUCKINGHAM-PI THEOREM

The parameters k_1 and k_3 in Eq. (4.20) were deduced as fluid flow parameters by means of complete set of dimensionless groups derived using the Buckingham-Pi theorem. The variables and dimensional constants believed to be involved in k_1 are ρ, μ, g, L, D, V and k_1. Thus the number of primary dimensions (M, L and θ) is

$$m= 3 \tag{F.1}$$

and the number of variables is

$$n= 8 \tag{F.2}$$

yielding

$$p= n-m = 5 \tag{F.3}$$

dimensionless groups according to the Buckingham-Pi theorem. The following dimensionless groups were found;

$$\pi 1 = \rho^a \mu^b V^c k_1 \tag{F.4}$$

$$\pi 2 = \rho^a \mu^b V^c g \tag{F.5}$$

$$\pi 3 = \rho^a \mu^b V^c P \tag{F.6}$$

$$\pi 4 = \rho^a \mu^b V^c L \tag{F.7}$$

$$\pi 5 = \rho^a \mu^b V^c D \tag{F.8}$$

in terms of the variables, ρ, μ and V. The dimensional equation corresponding to Eq. (F.4) is

$$M^0L^0\theta^0 = \left(\frac{M}{L^3}\right)^a \left(\frac{M}{L\theta}\right)^b \left(\frac{L}{\theta}\right)^c \left(\frac{L^2}{\theta}\right) \tag{F.9}$$

Applying the condition of dimensional homogeneity, the following equalities

$$\sum M = 0 = a + b \tag{F.10}$$

$$\sum L = 0 = -3a - b + c + 2 \tag{F.11}$$

$$\sum \theta = 0 = -b - c - 1 \tag{F.12}$$

were obtained with the solution

$$a = 1 \tag{F.13}$$

$$b = -1 \tag{F.14}$$

$$c = 0 \tag{F.15}$$

Thus, Eq. (F.4) becomes

$$\pi_1 = \left(\frac{\rho}{\mu}\right) k_1 \tag{F.16}$$

In the similar manner, the following dimensionless groups were deduced from Eqs. (F.5-8)

$$\pi_2 = \sqrt{\frac{\mu}{\rho V^5 g}} \tag{F.17}$$

$$\pi_3 = \frac{P}{\rho V^2} \tag{F.18}$$

$$\pi_4 = \frac{LV\rho}{\mu} \tag{F.19}$$

$$\pi_5 = \frac{DV\rho}{\mu} \tag{F.20}$$

For k_3, again the same procedure was used. The variables involved in k_3, the number of primary dimensions and the number of variables are the same. Thus the following dimensionless groups were found.

$$\pi 1 = \rho^a g^b P^c k_3 \tag{F.21}$$

$$\pi 2 = \rho^a g^b P^c \mu \tag{F.22}$$

$$\pi 3 = \rho^a g^b P^c L \tag{F.23}$$

$$\pi 4 = \rho^a g^b P^c V \tag{F.24}$$

$$\pi 5 = \rho^a g^b P^c D \tag{F.25}$$

in terms of the variables, ρ, g and P. The dimensional equation corresponding to Eq. (F.21) is

$$M^0L^0\theta^0 = \left(\frac{M}{L^3}\right)^a \left(\frac{L}{\theta^2}\right)^b \left(\frac{M}{L\theta^2}\right)^c \left(\frac{1}{L}\right) \tag{F.26}$$

Applying the condition of dimensional homogeneity, the following equalities

$$\sum M = 0 = a + c \tag{F.27}$$

$$\sum L = 0 = -3a + b - c - 1 \tag{F.28}$$

$$\sum \theta = 0 = -2b - 2c \tag{F.29}$$

were obtained with the solution

$$a = 1 \tag{F.30}$$

$$b = -1 \tag{F.31}$$

$$c = 1 \tag{F.32}$$

Thus, Eq. (F.21) becomes

$$\pi_1 = \left(\frac{\rho P}{g}\right) k_3 \tag{F.33}$$

In the similar manner, the following dimensionless groups were deduced from Eqs. (F.22-25)

$$\pi_2 = \frac{\rho^{1/2} g}{P^{3/2}} \mu \tag{F.34}$$

$$\pi_3 = \frac{\rho g L}{P} \tag{F.35}$$

$$\pi_4 = \frac{\rho^{1/2} V}{P^{1/2}} \tag{F.36}$$

$$\pi_5 = \frac{\rho g D}{P} \tag{F.37}$$